TAMPERE UNIVERSITY OF TECHNOLOGY

BASHIR AHMED SIDDIQUI

SIMULINK-BASED ACQUISITION UNIT FOR GALILEO E1 CBOC MODULATED SIGNALS

MASTER OF SCIENCE THESIS

Examiners: Docent Simona Lohan
M.Sc. Danai Skournetou

Examiners and topic approved in the Computing and Electrical Engineering Faculty Council meeting on 4th November, 2009

Abstract

TAMPERE UNIVERSITY OF TECHNOLOGY

Degree Program in Information Technology, Department of Communication Engineering

Siddiqui, Bashir Ahmed: Simulink-Based Acquisition Unit for Galileo E1 CBOC Modulated Signals

Master of Science Thesis, 78 Pages

March 2010

Examiners: Dr. Docent Elena-Simona Lohan and M.Sc. Danai Skournetou

Funding: Academy of Finland and EU FP7-funded project Galileo Ready Advanced Mass Market Receiver (GRAMMAR)

Keywords: Galileo, Acquisition, Composite Binary Offset Carrier (CBOC), E1 band, Simulink

At the moment, Global Positioning System (GPS) is the only positioning system with global coverage. Currently, there are efforts to modernize GPS with the aim of improving its performance. Meanwhile, Europe is developing its own satellite positioning system, GALILEO. In order to provide interoperability with GPS and globally available navigational systems, new modulation techniques have been introduced. Multiplexed Binary-Offset-Carrier (MBOC) modulated signals are the main candidates for the future Galileo Open Services (OS) and modernized GPS L1C signals. Spreading waveforms corresponding to pilot and data components can be formed in a number of ways, including Composite Binary Offset Carrier (CBOC) and Time-Multiplexed Binary Offset Carrier (TMBOC). CBOC is considered here because CBOC has been selected for Galileo E1 OS signals in the most recent Galileo SIS-ICD of 2008 [1].

This new composition of E1 signal allows different techniques for acquiring the signal, i.e. data-only channel, pilot-only channel and joint data and pilot channel. The

MBOC(6,1,1/11) power spectral density (PSD) has better performance than SinBOC(1,1) power spectral density because it is a mixture of BOC(1,1) spectrum and BOC(6,1) spectrum. MBOC modulation schemes also bring new challenges due to additional side lobes in the envelope of the Autocorrelation Function (ACF) compared with the traditional BPSK modulation used in the basic GPS signals, which make the signal acquisition process challenging. In order to deal with the side lobes, the steps 'Δt_{bin}' for searching the time-bin search space should be chosen carefully.

The goal of this thesis has been to develop an acquisition unit based on CBOC reference code and analyze the performance of new acquisition unit in terms of acquisition performance because MBOC signal has better power spectral density compared to SinBOC(1,1) signal. A brief study about the choice of the time-bin step 'Δt_{bin}' for searching the time-frequency window has been studied. Three different strategies have been used to acquire the signal and results are presented for each approach. The switching architecture model has introduced in the transmitter part which operates at dual frequency are also addressed under the scope of this thesis. The simulations are carried out with an own developed Simulink model for Galileo OS E1 signals, based on the most recent Galileo Signal-in-Space Interface Control Documentation.

Conclusions are drawn with respect to the performance deterioration of a reference SinBOC(1,1) receiver compared to a reference CBOC receiver, and also with respect to different techniques used for acquiring the signal. Comparisons between the infinite bandwidth (theoretical case, typically used in literature) and a limited front-end filter bandwidth of 3 MHz (double-sided bandwidth) are also made. The choice of significant detection threshold in order to detect the signal properly and the performance degradation of the CBOC reference receiver when using switching architecture model in terms of detection probability are also presented.

Preface

The research work reported in this thesis has been carried out during the years 2009-2010 at the Department of Communications Engineering, Tampere University of Technology, Finland. The work has been supported by the Academy of Finland-funded project “Digital Processing Algorithms for Indoor Positioning Systems” and the EU FP7-funded project under grant agreement number 227890 “Galileo Ready Advanced Mass Market Receiver (GRAMMAR)”.

I would like to extend my profound gratitude to my supervisors Prof. Markku Renfors and Dr. Simona Lohan for their enthusiastic encouragement, valuable guidance, constant support and patience during the whole working period, and providing me the opportunity to work on a stimulating research topic. I am sincerely grateful to M.Sc. Danai Skournetou for her fruitful technical discussion, helpful comments and infinite tolerance with the incomplete draft of this thesis. I am also thankful to M.Sc. Muhammad Zahid and Zhang Jie for their friendly and generous support during the research work.

I am profoundly grateful to all of my friends from Tampere for creating such a cheerful and unforgettable time together. Last but not least, I wish to express my deep gratitude and warmest thanks to my parents, brother and sisters for their unconditional support, endless love and encouragement during my studies.

Tampere, March 2010.

Bashir Ahmed Siddiqui

Table of Contents

List of Acronyms

ACF	Autocorrelation Function
AltBOC	Alternative BOC
ARNS	Aeronautical Radio Navigation Services
AWGN	Additive White Gaussian Noise
B&F	Betz & Fishman
BOC	Binary Offset Carrier
BPSK	Binary Phase Shift Keying
C/A	Coarse/Acquisition
CBOC	Composite BOC
CDMA	Code Division Multiple Access
CFAR	Constant False Alarm Rate
CNR	Carrier-to-Noise Ratio
CS	Commercial Services
DoD	Department of Defense
ESA	European Space Agency
FFT	Fast Fourier Transform
GLONASS	GLobal Orbital NAvigation Satellite System
GNSS	Global Navigation Satellite System
GPS	Global Positioning System
I & D	Integrate and Dump

LOS	Line-Of-Sight
MBOC	Multiplexed BOC
MEE	Mean Error Envelope
OS	Open Services
PDF	Probability Density Function
PRN	Pseudo Random Number
PRS	Public-Regulated-Services
PSD	Power Spectral Density
RHCP	Right-Hand Circular Polarization
RNSS	Radio Navigation Satellite Services
RMSE	Root Mean Squared Error
SAR	Search-And-Rescue-services
SB	Side Band
SinBOC	Sine BOC
SIS-ICD	Signal In Space Interface Control Document
SoL	Safety-of-Life-services
STF	Galileo Signal Task Force
SV	Satellite Vehicle
TMBOC	Time Multiplexed BOC
UAL	Unsuppressed Adjacent Lobes

List of Symbols

Δ	Mean Absolute Error
Δf_{bin}	Frequency Bin Length
Δt_{bin}	Time Bin Length
$\widehat{\tau}_{LOS}$	Estimated LOS Delay Error
τ_{LOS}	True LOS Delay Error
τ_i	Channel Delay Introduced by i-th Path
τ	Channel Delay
σ^2	Variance
γ	Detection Threshold
$\delta(t)$	Dirac Pulse
N_{BOC1}	BOC Modulation Order for SinBOC(1,1)
N_{BOC2}	BOC Modulation Order for SinBOC(6,1)
Nc	Coherent Integration Length in Code Epochs (or ms)
Nnc	Non-Coherent Integration Length in Blocks
Ns	Oversampling Factor
P_d	Detection Probability
P_{fa}	False Alarm Probability
S_F	Spreading Factor
T_c	Chip Period; 1/ *fc*
T_{sym}	Symbol Period

Z	Correlation Output
c	Speed of Light
fc	Carrier Frequency
fIF	Intermediate Frequency
fs	Sampling Frequency
*f*sc	Subcarrier Frequency
m	Nakagami-m Fading Parameter

Chapter 1

Introduction

In recent years, positioning and navigation based applications have seen impressive growth due to their application in different fields, e.g., land transportation, civil aviation, maritime commerce, surveying and mapping, construction, mining, agriculture, earth sciences, electric power systems, telecommunications, and outdoor recreational activities. Due to the increasing demand in the field of navigation, several countries started to develop or modernize their own navigational systems. For instance, the European Union is developing GALILEO, the Russian GLONASS is under maintenance phase towards modernization and the China is designing COMPASS to meet the positioning needs. During the past couple of years, the global positioning system is being modernized with the addition of new frequency bands for civilian and military usage. The ambition of these projects is to increase the accuracy and availability for all users.

1.1 Motivation and Background

The Navstar Global Positioning System (GPS) is currently the only fully operational global navigation satellite system (GNSS) available. Officially named as NAVSTAR GPS, it was developed by United States (US) Department of Defense (DoD) and declared fully operational on July, 1995. It uses a constellation of 24 satellites that provides reliable positioning, navigation and timing services to all users worldwide. The primary goal of the GPS was to serve military purposes [2] but later on it has been widely used for civilian applications, such as from personal navigation to vehicular application, land and maritime transportation to aircraft navigation and search and rescue operation to safety of life execution. However, because GPS is military controlled, there is no guarantee of its availability. In case GPS system is switched off,

the users of it will be exposed and experience the discontinuity of its service. This is one of the reasons, that during 90's, the European Union decided to develop its own global satellite navigation system under civilian control [5].

The Galileo system will have a constellation of 30 satellites, which will be placed on three different orbital planes at an altitude of 23 222 Km above the Earth. The Galileo system will transmit on four different frequency bands and offer a variety of services like Open Service free of user charge for mass markets, Commercial Service (CS) which offers more precise positioning services, Public Regulated Service (PRS) allocated for police or defense use with controlled access, Safety-of-Life Service (SoL) and Search and Rescue Service (SAR) [5]. In this thesis, we will only focus on E1 OS signal.

With the advent of the new global navigation satellite system i.e. European Galileo, Russian GLONASS and Chinese Compass, new modulation schemes have been introduced in order to provide interoperability with GPS and globally available navigational systems. The agreement reached in 2004 by United States and European Commission (EC) focusing on the Galileo and GPS coexistence stated that Binary Offset Carrier (BOC) modulation would be the common baseline structure for signal in space (SIS). Considering the recent activities carried out by the Galileo signal task force (STF) jointly to US experts in the Working Group A, it came out that the Multiplexed BOC could be a good candidate for both GPS and Galileo satellites [3].

In fact, on the 26th of July 2007 US and EC announced their decision to jointly implement the MBOC on the Galileo open service and the GPS IIIA civil signal [5]. Different time waveforms can be used to produce MBOC power spectral density (PSD), including Composite BOC and Time-Multiplexed BOC. CBOC is considered here because CBOC has been selected for Galileo E1 OS signals in the most recent Galileo SIS-ICD of 2008. This new modulation is the sum (or difference) of two Sine-BOC (or SinBOC) sub-carrier waves. The one used in E1 band is called Composite Binary Offset Carrier modulation and it is denoted as CBOC(6,1,1/11), or, briefly, as CBOC(+) or CBOC(-), which is the sum (or difference) of SinBOC(1,1) and SinBOC(6,1), respectively. The factor 1/11 stands for the power fraction from SinBOC(6,1). The

CBOC(+) modulation is employed for the data channel (or E1-B), while CBOC (-) is used for the pilot channel (or E1-C) [4].

Acquisition is the first stage in the digital signal processing section of a GNSS receiver that aims to get rough estimates of the Doppler frequency and code delay of the received signals. In the acquisition process, the received signal is correlated with locally generated replica of the spreading code with different code delays and frequencies, in order to provide correct estimates of the code phase and Doppler frequency of the satellite signals. The E1 OS signal is composed of two channels: the data and the pilot channel. The former carries the navigation data whereas the latter is data-free channel. This new composition of E1 signal allows one to choose different techniques in order to acquire the signal. The presence of pilot channel in E1 band allows the receivers to have the choice to acquire the data or the pilot component, or both. Since the new modulation CBOC(6,1,1/11) combines two sub-carrier wave components, the acquisition can be done either with CBOC modulated reference code, which is the same as transmitted signal, or with SinBOC(1,1) modulated reference code, since more than 90 percent power is in SinBOC(1,1) component [16].

The Power spectral density of MBOC signal is a combination of SinBOC(1,1) and SinBOC(6,1) power spectra (i.e., including both pilot and data channel components). The contribution of the BOC(6,1) subcarrier increases the amount of power on higher frequencies, which leads to signals with narrower autocorrelation function (ACF) and then yielding better performance at the receiver level [3]. Therefore, two types of receiver are used here; one with CBOC reference code and one with SinBOC(1,1) reference code. More precisely, the reference CBOC receiver correlates the incoming CBOC-modulated waveform with a reference CBOC-modulated waveform (i.e., transmit and receive modulations are the same). The reference SinBOC(1,1) receiver correlates the incoming CBOC modulated waveform with a reference SineBOC(1,1)-modulated waveform. In the second approach, the implementational complexity is lower and thus, it is more suitable for mass-market receivers.

One challenge for the acquisition task is the new modulation type proposed for Galileo and modernized GPS signals. The normalized ACF of CBOC modulated signals may have ambiguities within ± 1 chip interval around the maximum peak [17] and therefore, the choice of the step for searching the time bin 'Δt_{bin}' is even more crucial.

1.2 Thesis Objectives

This thesis work has been carried out within 2 research projects of the Department of Communications Engineering (DCE) at Tampere University of Technology: the Academy of Finland-funded project "Digital Processing Algorithms for Indoor Positioning Systems" and the EU FP7-funded project under grant agreement number 227890 "Galileo Ready Advanced Mass Market Receiver (GRAMMAR)". The main objective of this thesis is to analyze the effects of CBOC modulations on signal acquisition stage. The goals have been to implement and analyze the performance of CBOC reference receiver, variable time-bin steps (steps 'Δt_{bin}' for searching time-bin window) and switching architecture (transmitter operates at dual frequency i.e. E1 and E5 bands) model for signal acquisition.

1.3 Thesis Contributions

The primary contributions of this thesis are summarized as follows:

- Implementation of a new acquisition unit based on CBOC reference signal.
- Modification of the existing acquisition block in such a way that also steps higher than 1 BOC/CBOC sample are allowed.
- Implementation of different acquisition strategies i.e. data-only, pilot-only and joint data and pilot channel to acquire the signal.
- Implementation of switching architecture model at transmitter unit.

1.4 Thesis Outline

The thesis is organized as follows:

- In Chapter 2, a brief overview of Galileo system and signals is presented; in particular, the focus is put on BOC modulation. The BOC modulation is explained in detail, followed by a description of MBOC and CBOC

modulations. In the end, detailed discussion about E1 OS signals characteristics are presented.

- In Chapter 3, the acquisition principles in GNSS receiver are illustrated. The false alarm and detection probabilities are also discussed here.

- In Chapter 4, detailed Simulink model developed at TUT is described, further discussion explains the implementation of new block and modification of existed block in the model.

- In Chapter 5, Simulink-based simulation results are presented and a discussion on the results is included.

- In Chapter 6, Matlab-based simulation results are presented and comparisons with Simulink results have been made.

- Chapter 7 draws the conclusion of this research and provides recommendation regarding the future work.

Chapter 2

Emerging Galileo System and CBOC Modulation

Global Navigation Satellite System is a specific term for a satellite navigation system that provides autonomous geo-spatial positioning with global coverage. The Global Navigation Satellite System is being progressively used throughout the world in order to overcome many of the limitations of today's air navigation infrastructure. GNSS allows a small electronic receiver to compute position (longitude, latitude and altitude) with accuracy of few meters using time signals transmitted from satellites.

Nowadays, United States Global Positioning System [7] is the only fully functional, available global navigation system. The Russian GLONASS is a GNSS under the maintenance phase towards modernization. Russia accelerated the modernization program with a goal of restoring global coverage by 2012 [9]. People's Republic of China has decided to expand its regional BEIDOU navigation system into global COMPASS navigation system by 2015 [8]. The European Union's GALILEO positioning system is a GNSS in initial deployment phase, scheduled to be operational in 2013. This chapter starts describing the Galileo system and its signal characteristics, then it discusses BOC and CBOC modulations and in the end, E1 signal characteristics are explained in detail.

2.1 Introduction to Galileo System

Galileo is a global navigation system currently being built by a joint initiative of the European Commission and the European Space Agency (ESA) in order to provide Europe its own independent global civilian controlled satellite navigation. It was named after the Italian astronomer Galileo Galilei. The European positioning system is

officially referred to as just Galileo. The €3.4 billion project [6] is an alternative and complementary to the U.S. Global Positioning System and the Russian GLONASS.

Galileo system will provide a highly accurate, guaranteed global positioning service which will lead to a fully civilian controlled global satellite navigation system. It will be an autonomous system inter-operable with GPS and globally available. A user will be able to measure position using the same receiver with the help of at least four satellites in any combination. Moreover, Galileo system will provide real-time positioning accuracy down to the meter range, which will be a milestone for a publicly available system [5]. It is based on the same technology as GPS, i.e., "Direct Sequence Code Division Multiple Access (DS-CDMA)". Galileo aims to provide more precise measurements than the GPS and GLONASS including the height (altitude) above sea level and better positioning services at high latitudes.

2.1.1. Galileo System Overview

The Galileo system will be based on a constellation of 30 satellites (27 operational and 3 spares), orbiting around 3 circular Medium Earth Orbit (MEO) planes at an altitude of 23 222 Km, and at an inclination of 56 degree. The placement of satellites is made in such a way that each plane will contain nine operational satellites, equally spaced, 40 degrees apart, plus one spare satellite to replace any of the operational satellites in case of failure. The Galileo navigation satellites will provide good coverage even at latitudes up to 75 degrees north, which correspond to the North Cape and beyond. The basic idea is that at any time four satellites are located above the horizon for all points of the Earth [1].

The following Galileo satellite-only services [1][11] will be provided worldwide and independently from other systems by combining Galileo signals-in-space:

- The Open Service results from a combination of signals, free of user charge, and it provides position and timing performance competitive with other GNSS systems.

- The Safety-of-Life Service improves the open service performance through the provision of timely warnings to the user when the latter fails to meet certain margins of accuracy. It will be mostly used for professional applications.

- The Commercial Service provides access to two additional signals, in order to allow a higher data throughput rate and to enable users to improve accuracy. It will provide high accuracy and guaranteed service.

- The Public Regulated Service provides position and timing to specific users requiring a high continuity of service, with controlled access. Two PRS navigation signals with encrypted ranging codes and data will be available.

- The Galileo support to the Search and Rescue Service represents the contribution of Europe to the international COSPAS-SARSAT co-operative effort on humanitarian Search and Rescue activities. Galileo satellites will be able to pick up signals from emergency beacons carried on ships, planes or persons and ultimately send these back to national rescue centers. From this, a rescue centre can know the precise location of an accident [13].

2.1.2. Galileo Signal Characteristics

The Galileo navigation signals are transmitted in the four frequency bands indicated in Figure 2.1. These frequency bands are E5a, E5b, E6 and E1. Different frequencies have been assigned to the Galileo system depending on the service type. Frequency bands are divided into lower L-band (corresponding to E5a and E5b frequency bands with carrier frequencies, fc = 1176.45 MHz at E5a and fc = 1207.14 MHz at E5b), middle L-band (i.e., E6 frequency band with fc = 1278.75 MHz) and upper L-bands (E2-L1-E1 band with fc = 1575.42 MHz) [10]. It can be noticed that both GPS and Galileo use certain identical carrier frequencies. This guarantees the ability to attain interoperability between the two systems [11]. OS is planned to operate on the E5a, E5b and E1 carriers, SAR on the E5a, E5b and E1 carriers, CS on the E5b and E6 carriers, and PRS on the E6 and E1 [10].

The Galileo frequency bands have been selected in the allocated spectrum for Radio Navigation Satellite Services (RNSS) and in addition to that, E5a, E5b and

E1 bands are included in the allocated spectrum for Aeronautical Radio Navigation Services (ARNS), employed by Civil-Aviation users, and allowing dedicated safety-critical applications [1].

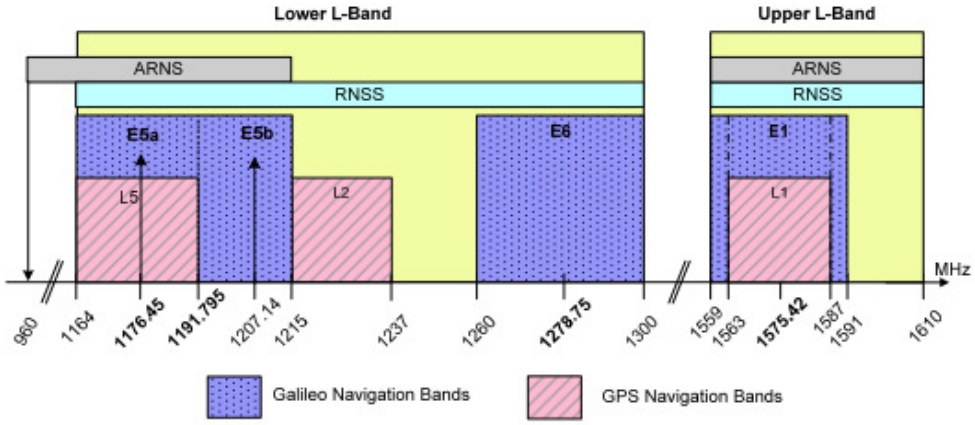

Figure 2.1: *Galileo signal in space [1].*

A summary of Galileo signal specifications, based on current standards [1] is shown in Table 2.1. Galileo satellite transmits six different navigation signals: E1, E6, E5, E5a and E5b signals. Table 2.1 also shows the carrier frequencies of all the signals. Note that E5a and E5b signals are part of E5 signal in its full bandwidth.

Table 2.1: *Carrier frequency per signals.*

Signal	Carrier Frequency (MHz)
E1	1575.420
E6	1278.750
E5	1191.795
E5a	1176.450
E5b	1207.140

Table 2.2 shows the receiver bandwidths centered on the carrier frequencies of Table 2.1. Since Galileo has longer spreading codes than GPS, wider receiver bandwidth is required. These are the nominal bandwidths specified in the standardization documents; however, for mass-market applications, much lower bandwidths may be employed.

Table 2.2: *Galileo Signal Receiver Reference Bandwidth.*

Signal	**Receiver Reference Bandwidth (MHz)**
E1	24.552
E6	40.920
E5	51.150
E5a	20.460
E5b	20.460

The ranging codes are built from the primary and secondary codes by using a tiered codes construction. The code length for six different signals which Galileo transmits is given in Table 2.3.

Table 2.3: *Code Lengths for Different Signals.*

Signal Component	**Tiered Code Length (ms)**	**Code Length (chips)**	
		Primary	**Secondary**
E5a-I	20	10230	20
E5a-Q	100	10230	100
E5b-I	4	10230	4
E5b-Q	100	10230	100
E1-B	4	4092	N/A
E1-C	100	4092	25

The most important characteristics of the Galileo signals, in comparison with the GPS signals, are the different modulation types and code lengths. The code length for the E1 signals is 4092 chips with 1.023 MHz chip rate for the pilot channel. A secondary code of length 25 chips extends the repetition interval to 10 ms. For the E5 signals, the code length is decided to be as high as 10230 chips. The multiplexing scheme here means the modulation type by which two signals are combined. For the E5 signals, the multiplexing scheme is Alternative BOC(15,10), and for the E1 signals, it is addition and subtraction of SinBOC(1,1) and SinBOC(6,1) for CBOC Data and CBOC Pilot, respectively [1].

Introduction of longer codes and new types of modulations are the main differentiating features of Galileo compared to GPS. For many years, SinBOC(1,1) has been the candidate modulation type for the Galileo OS signal in the E1 band [15]. Recently, the GPS-Galileo working group on interoperability and compatibility has recommended MBOC modulation that would be used by GALILEO for its Open Service signal at E1 frequency, and also by GPS for its modernized L1 Civil (L1C) signal [16]. The spreading codes for Galileo systems are pseudorandom data streams, whose design depends on the desired correlation properties and the acquisition time. The code length for the OS signal is 4092 chips, which is four times higher than the GPS Coarse Acquisition (C/A) code length of 1023 chips. Longer codes help to reduce the cross-correlation levels, but increase the acquisition time. Since the chip rate of 1.023 MHz is the same for Galileo OS and GPS C/A signals, a spreading factor of 1023 is used in both cases. This means that Galileo employs long codes, that is codes that are different from one symbol to another.

2.2 BOC Modulation

BOC modulation is a square sub-carrier modulation, where a signal is multiplied by a rectangular subcarrier of frequency $f$sc, which splits the spectrum of the signal into two parts [17][18]. Typically, the sine and cosine BOC modulations are defined via two parameters BOC(m, n) [17]. These two parameters are related to the reference 1.023 MHz frequency as follows: $m = f$sc/1.023 and $n = f$c/1.023, where fc is the chip rate, both $f$sc and fc are expressed in MHz here. There are several variants of BOC modulation: SinBOC [17], CosBOC [17], AltBOC [10] and MBOC [10]. BOC stands both for SinBOC modulation, and that the BOC notation is usually used within this thesis (for simplicity reason).

A sine BOC modulation is similar to Manchester code [19], that is, in digital domain, a '+1' is encoded as a '+1 -1' sequence, and a '0' is encoded as a '-1 +1' sequence. From the point of view of the equivalent baseband signal, the BOC modulation can be defined by a single parameter, known as BOC modulation order:

$$N_{BOC} \triangleq 2\frac{m}{n} = 2\frac{fsc}{fc} \tag{2.1}$$

Here N_{BOC} should be an integer number, therefore m and n should be chosen in a way that BOC order remains integer i.e., for SinBOC(1,1), the modulation order $N_{BOC} = 2$. In the same way, the modulation order $N_{BOC} = 12$ for SinBOC(6,1). If modulation order $N_{BOC,}$ chip rate and the carrier frequencies are known, passband signal can be easily reconstructed.

The SinBOC-modulated signal x(t) can be seen as the convolution between a SinBOC waveform $S_{SinBOC}(t)$ and a modulating waveform d(t), as follows [20]

$$x(t) = \sum_{n=-\infty}^{+\infty} b_n \sum_{k=1}^{S_F} c_{k,n} s_{SinBOC}(t - nT_{sym} - kT_c)$$

$$= s_{SinBOC}(t) \otimes \sum_{n=-\infty}^{+\infty} \sum_{k=1}^{S_F} b_n c_{k,n} \delta(t - nT_{sym} - kT_c) \triangleq s_{SinBOC(t)} \otimes d(t) \qquad (2.2)$$

where $\otimes$ is the convolution operator, d(t) is the spread data sequence, b_n is the n-th complex data symbol (in case of a pilot channel, it is equal to 1), T_{sym} is the symbol period, $c_{k,n}$ is the k-th chip corresponding to the nth symbol, $T_c = 1/fc$ is the chip period, S_F is the spreading factor ($S_F = T_{sym}/T_c$), and $\delta(t)$ is the Dirac pulse. The signals used in GPS and Galileo are wideband signals. The signal x(t) shown in Equation 2.2 is a wideband signal, that is, a signal spread by a pseudorandom (PRN) sequence.

According to its original definition in [17], the SinBOC waveform $S_{SinBOC}(t)$ is defined as:

$$s_{SinBOC}(t) = sign(\sin(\frac{\pi t N_{BOC}}{T_c})), 0 \le t \le T_c \qquad (2.3)$$

where sign(.) is the signum operator. Since, the above waveform is a sequence of +1 and −1, it can also be written as:

$$s_{SinBOC}(t) = P_{T_{B1}}(t) \otimes \sum_{i=0}^{N_{BOC}-1} (-1)^i \delta(t - iT_{B1}) \qquad (2.4)$$

where $P_{T_{B1}}(.)$ is the rectangular pulse of amplitude 1 and support $T_{B1} = T_c / N_{BOC}$. Time domain waveforms for SinBOC(1,1) are shown in Figure 2.2.

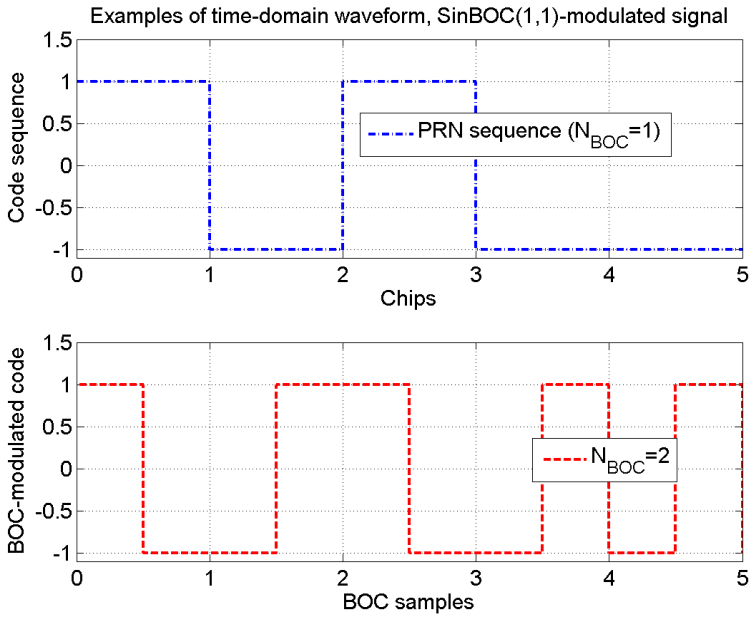

Figure 2.2: *Examples of time-domain waveform for SinBOC(1,1). Upper plot: PRN Sequence; Lower plot: SinBOC(1,1) modulated waveform.*

The SinBOC(1,1) modulation is part of the SinBOC(m,n) family, where the length of one subcarrier period equals one Pseudo-Random Noise (PRN) chip duration. To analyze its impact on signal tracking, a few details are included here. SinBOC(m,n) modulation splits the usual BPSK(n) spectrum into two symmetric side lobes centered at ±fsc MHz around the carrier frequency as seen in Figure 2.3. This allows a wider spectral occupancy. The SinBOC(m,n) PSD envelope is given by [17]:

$$G_{SinBOC(1,1)}(f) = fc\left(\frac{\sin\left(\frac{\pi f}{2fc}\right)\sin\left(\frac{\pi f}{fc}\right)}{\pi f \cos\left(\frac{\pi f}{2fc}\right)}\right)^2 \tag{2.5}$$

The SinBOC(1,1) PSD envelope is shown in Figure 2.3 along with the BPSK(1) PSD envelope that characterizes the GPS C/A code modulation. The SinBOC(1,1) PSD has its side lobes on the zeros of the GPS C/A code PSD. Consequently, its spectrum is well separated from the spectrum of C/A signal. BOC modulation provides a simple and

effective way of moving the signal energy away from band center, offering a high degree of spectral separation from conventional phase shift keyed signals whose energy is concentrated near band center. The resulting split spectrum signal effectively enables frequency sharing, while it provides attributes that include simple implementation, good spectral efficiency, high accuracy, and enhanced multi-path resolution [17].

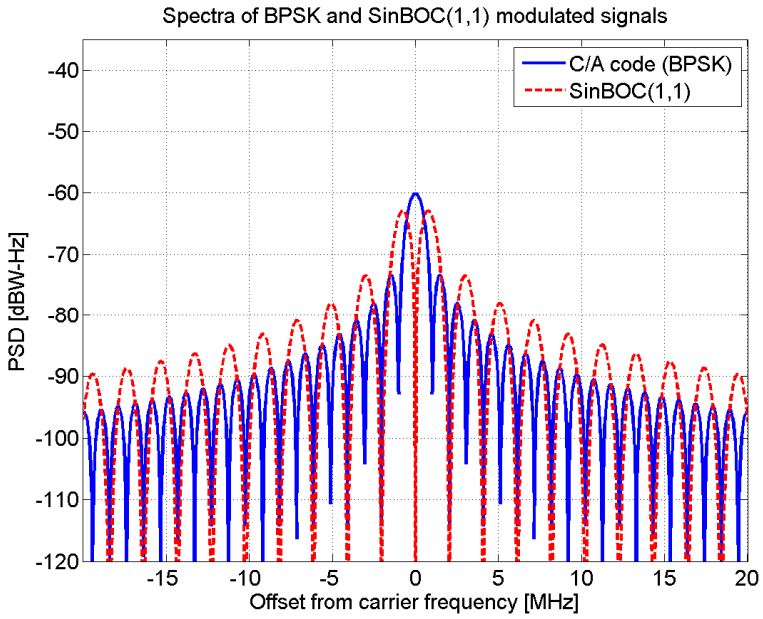

Figure 2.3: *SinBOC(1,1) and BPSK(1) normalized power spectral densities.*

2.3 MBOC Modulation

The power spectral density of MBOC signal can be obtained as a combination of SinBOC(1,1) and SinBOC(6,1) power spectra (i.e., including both pilot and data channel components). The notation introduced is MBOC(6,1,1/11), where the term (6,1) refers to the BOC(6,1), and the ratio 1/11 represents the power split between the BOC(1,1) and BOC(6,1) spectrum components as given by [3]

$$G_{MBOC}(f) = \frac{10}{11} G_{SinBOC(1,1)}(f) + \frac{1}{11} G_{SinBOC(1,1)}(f)$$

where $G_{MBOC(m,n)}(f)$ is the unit power PSD of a sine-phased BOC spreading modulation as defined in [17].

Figure 2.4 shows the PSDs of the BOC(1,1) and the MBOC(6,1,1/11). Due to SinBOC(6,1) component, extra lobes can be noticed at around ±6 MHz of the MBOC PSD as compared to SinBOC(1,1) case. The curves from Figure 2.4 were obtained with the Simulink model, and therefore, they are noisier than the theoretical curves reported in Figure 2.3, due to non-idealities of the used codes and channel imperfections. The curves in Figure 2.4 are centered to 0 frequency (baseband) here; however, if we talk about the modulated signal, they have to be shifted around the E1 carrier frequency.

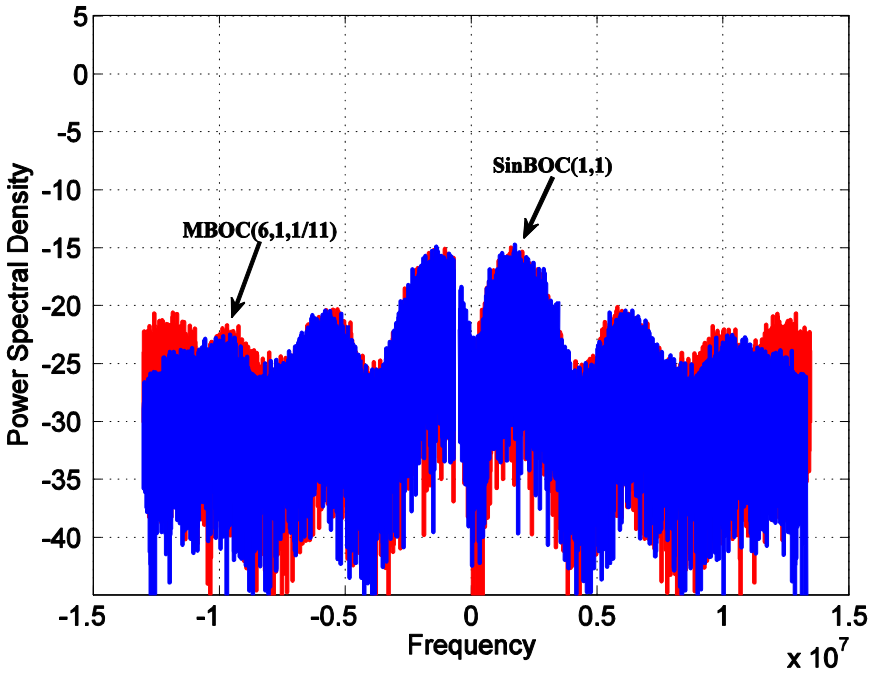

Figure 2.4: *Power Spectral Density for MBOC and SinBOC(1,1)-modulated signals.*

Spreading waveforms corresponding to pilot and data components can be formed in a number of ways, including Composite BOC (CBOC), which adds or subtracts BOC(6,1) spreading symbols at the appropriate power level with BOC(1,1) spreading symbols, and time-multiplexed BOC, which produces a spreading waveform containing BOC(1,1) spreading symbols, interspersed with the appropriate fraction of time of BOC(6,1) spreading symbols. In the following contexts, TMBOC and Composite BOC is described here but the focus has given to CBOC because it has been selected for Galileo E1 OS signals in the most recent Galileo SIS-ICD of 2008 [1].

2.3.1. TMBOC Implementation

In a TMBOC implementation, the whole signal is divided into blocks of N code symbols. Out of N code symbols M < N are SinBOC(1,1)-modulated, while the remaining N-M code symbols are SinBOC(6,1)-modulated [20]. Since different spreading time series can be used to form data and pilot components, the total signal power can be divided between the data and pilot components so many different implementations of TMBOC are possible. TMBOC has been selected for the modernized GPS signal L1C in L1 band [22].

2.3.2. CBOC Definition and Implementation

Composite BOC (CBOC) uses multilevel spreading symbols formed from the weighted sum of BOC(1,1) and BOC(6,1) spreading symbols, interplexed to form a constant modulus composite signal [16]. CBOC can be implemented using four-level spreading symbols formed by the weighted sum of SinBOC(1,1) and SinBOC(6,1) modulated code symbols [16][21]. A time domain representation of a CBOC implementation is shown in Figure 2.5 [22].

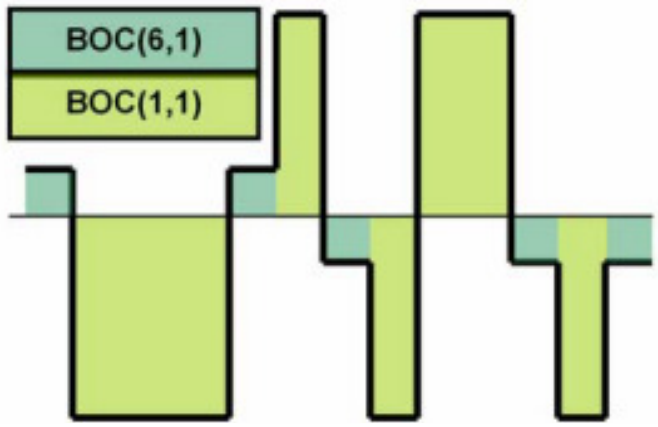

Figure 2.5: *Pseudo-random time multiplexing of BOC(6,1) and BOC(1,1) in the CBOC solution [22].*

Two different implementations of CBOC could be considered for a 50%/50% power split between data and pilot components [16].

- CBOC symbols could be used in both data and pilot channels, and formed from the sum of $\sqrt{10/11}$ SinBOC(1,1) symbols and $\sqrt{1/11}$ SinBOC(6,1). This is the variant currently selected in the SIS-ICD [1].

- Alternatively, CBOC symbols could be used on only the pilot components while leaving all the data component with SinBOC(1,1). In this case, CBOC is formed as the sum of $\sqrt{9/11}$ SinBOC(1,1) symbols and $\sqrt{2/11}$ SinBOC(6,1) symbols.

As defined in [23], CBOC can be implemented using three signals models:

- CBOC ('+')
- CBOC ('−')
- CBOC ('+/-')

The time waveforms of CBOC('+'), CBOC('-') and CBOC('+/-') along with the original PRN sequence are depicted in Figure 2.6.

Based on the BOC model and derivations of [20], CBOC('+') can be written as [36]:

$$S_{CBOC('+')}(t) = w_1 s_{SinBOC(1,1),held}(t) + w_2 s_{SinBOC(6,1),held}(t)$$

$$\sum_{i=0}^{N_{BOC1}-1} \sum_{k=0}^{\frac{N_{BOC2}}{N_{BOC1}}-1} (-1)^i c(t - i\frac{T_c}{N_{BOC1}} - k\frac{T_c}{N_{BOC2}})$$

$$+w_2 \sum_{i=0}^{N_{BOC2}-1} (-1)^i c(t - i\frac{T_c}{N_{BOC2}}) \qquad (2.6)$$

Where $N_{BOC1} = 2\,{fsc}/{fc}$ and N_{BOC2} is the BOC modulation order of the second stage, w_1 and w_2 represents the weighting factors. An example of weights, as given in [1] is w_1 = $\sqrt{10/11}$ and $w_2 = \sqrt{1/11}$. In equation 2.5, the first term represents SinBOC(1,1) modulated code and the second term represents SinBOC(6,1) modulated code. Above, c(t) defines the modulation waveform.

CBOC('-') modulation can be implemented by subtracting the weighted SinBOC(6,1) modulated symbol from the weighted SinBOC(1,1) modulated symbol [22]. This composite subtraction can be written as:

$$S_{CBOC('-')}(t) = w_1 s_{SinBOC(1,1),held}(t) - w_2 s_{SinBOC(6,1),held}(t) \tag{2.7}$$

CBOC('+/-') modulation can be implemented in a way that the weighted SinBOC(1,1) modulated symbol is summed with the weighted SinBOC(6,1) modulated symbol for even chips and the weighted SinBOC(6,1) modulated symbol is subtracted from the weighted SinBOC(1,1) modulated symbol for odd chips [22].

$$s_{CBOC('+/-')}(t) = \begin{cases} w_1 s_{SinBOC(1,1),held}(t) + w_2 s_{SinBOC(6,1)}(t) & even\ chips \\ w_1 s_{SinBOC(1,1),held}(t) - w_2 s_{SinBOC(6,1)}(t) & odd\ chips \end{cases}$$

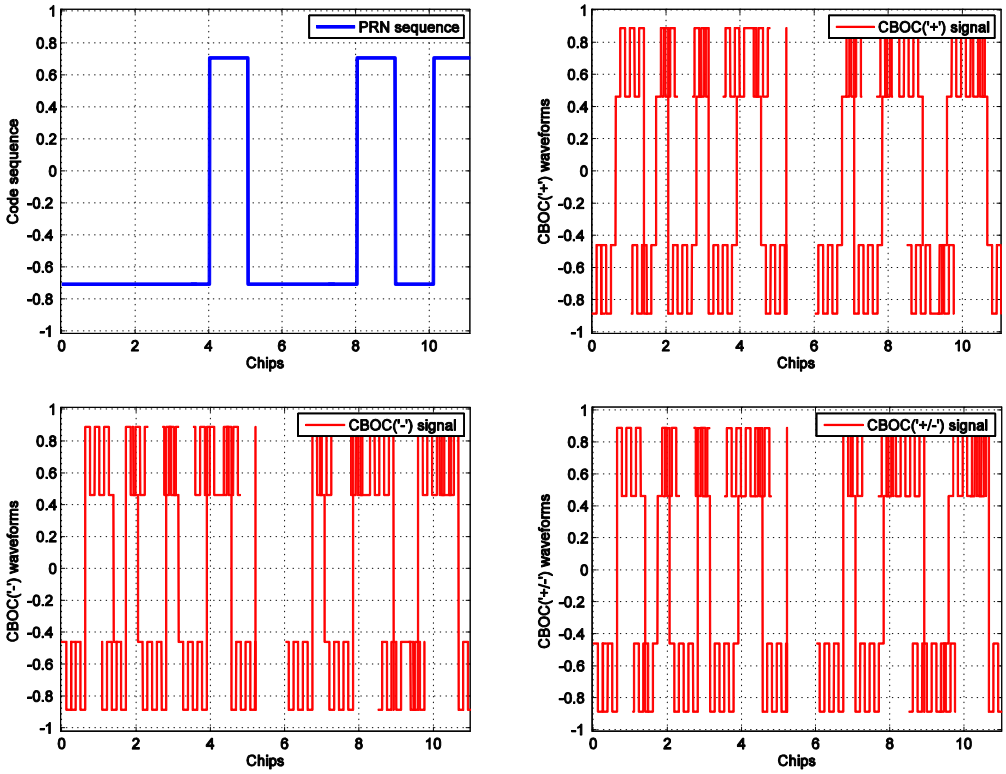

***Figure 2.6**: Examples of CBOC time waveforms. Upper left plot: PRN sequence; Upper right plot: CBOC('+') modulated waveform; Lower left plot: CBOC('-') modulated waveform; Lower right plot: CBOC('+/-') modulated waveform.*

Figure 2.7 shows the correlation function of each of the CBOC types. The sign of the SinBOC(6,1) component also shapes the correlation function [20].

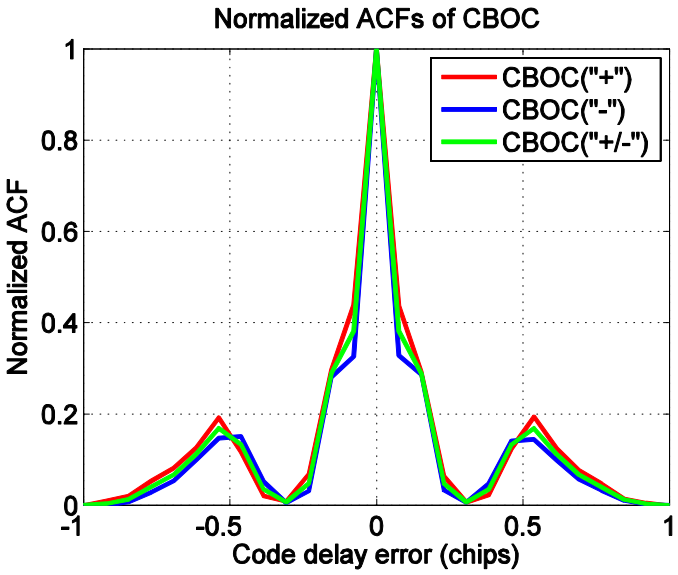

Figure 2.7: *Normalized ACFs of CBOC(+), CBOC('-') and CBOC('+/-').*

Based on the above figure, CBOC(-) has the sharpest main lobe peak, and therefore is the most suitable for high-accuracy tracking. This might have been one of the reasons for which CBOC(-) was selected as the modulation for the pilot E1-C channel. The data channel uses a CBOC(+) modulation [1].

2.4 Why CBOC

The agreement reached in 2004 by United States and European Commission focusing on the Galileo and GPS coexistence clearly stated that BOC(1,1) is to be the common baseline structure for signal in space (SIS). In addition, the same agreement paved the way for common signal optimization with the goal to provide improved performance as well as considerable flexibility to receiver manufacturers. Therefore, EC and US started to analyze possible innovative modulation strategies in the view of Galileo E1 OS optimization and for the future L1C signals of the new generation GPS satellites. Considering the recent activities carried out by the Galileo signal task force (STF) jointly to US experts in the Working Group A, it came out that the MBOC could be a good candidate for both GPS and Galileo satellites. In fact, on the 26th of July 2007 US and EC announced their decision to jointly implement the MBOC on the Galileo open service and the GPS IIIA civil signal [3].

In the context of the integration between wireless communication and satellite navigation, one of the major problems is that usually the GNSS receiver has to work in a critical environment characterized by a heavy presence of multi-path or interference sources. The new MBOC modulation has been studied with the goal to create a signal more robust with respect to multi-path, bringing the high performance of Galileo in situations in which the present BOC(1,1) shows limitations. The European approach to the MBOC implementation consists in adding in time a BOC(1,1) and a BOC(6,1), defined as composite BOC modulation. CBOC signal structure allows the receivers to obtain high performance in terms of multi-path rejection and tracking [21]. The contribution of the BOC(6,1) subcarrier brings in an increased amount of power on higher frequencies, which leads to signals with narrower correlation functions and then yielding better performance at the receiver level. This is mainly due to a higher transition rate brought by the BOC(6,1) on top of the BOC(1,1). All these considerations together with the major advantages in terms of better tracking performance and multi-path rejections capabilities clearly justify the selection of the CBOC as implementation of the agreed MBOC [3].

2.5 E1 Signal Description

E1 CBOC signal generation can be visualized in Figure 2.8 [1]. The E1 CBOC signal components are generated as follows [1]:

- $e_{E1\text{-}B}$ from the I/NAV navigation data stream $D_{E1\text{-}B}$ and the ranging code $C_{E1\text{-}B}$, then modulated with the sub-carriers $SC_{E1\text{-}B,a}$ and $SC_{E1\text{-}B,b}$.

- $e_{E1\text{-}C}$ (pilot component) from the ranging code $C_{E1\text{-}C}$ including its secondary code, then modulated with the sub-carriers $SC_{E1\text{-}C}$,a and $SC_{E1\text{-}C,b}$.

Mathematical formulations of these components are given in equation 2.9 [1]

$$e_{E1-B}(t) = \sum_{i=-\infty}^{+\infty} \left[c_{E1-B,[i]} L_{L1-B} D_{E1-B,[i]_{DC_{E1-B}}} P_{T_{c,E1-b}}(t - iT_{c,E1-B}) \right]$$
$$e_{E1-C}(t) = \sum_{i=-\infty}^{+\infty} \left[c_{E1-C,[i]} L_{L1-C} P_{T_{c,E1-C}}(t - iT_{c,E1-C}) \right] \quad (2.8)$$

where $P_{T_c}(.)$ is the rectangular pulse of amplitude 1. The parameters α and β are chosen such as that the combined power of the $sc_{E1-B,b}(t)$ and the $sc_{E1-C,b}(t)$ subcarrier components equals to 1/11 of the total power of $e_{E1\text{-}B}$ plus $e_{E1\text{-}C}$, before application of any bandwidth limitation. This yields:

$$\alpha = \sqrt{\frac{10}{11}} = w_1 \text{ and } \beta = \sqrt{\frac{1}{11}} = w_2$$

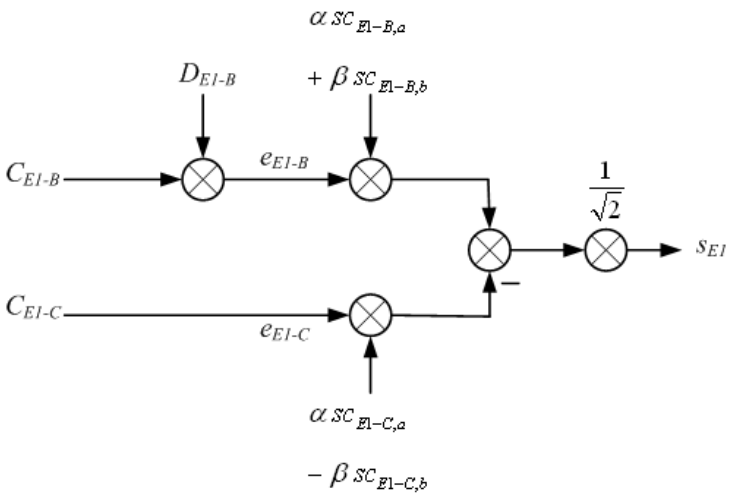

Figure 2.8: *Modulation Scheme for the E1 CBOC Signal.*

Galileo satellites transmit ranging signals for the E1 signal with the chip rates and sub-carrier rates defined in the following Table 2.4 [1].

Table 2.4: *E1 CBOC Chip- and Subcarrier Rates.*

Component (Parameter Y)	**Sub-carrier Type**	**Sub-carrier Rate $R_{S,E1\text{-}Y,a}$ (MHz)**	**$R_{S,E1\text{-}Y,a}$ (MHz)**	**Ranging Code Chip- Rate $R_{C,E1\text{-}Y}$ (Mcps)**
B	CBOC, in-phase (CBOC(+))	1.023	6.138	1.023
C	CBOC, anti-phase (CBOC(-))	1.023	6.138	1.023

After channel encoding, the navigation data message stream is transmitted with the symbol rate as stated in Table 2.5 [1].

Table 2.5: *E1 Symbol Rates.*

Component (Parameter Y)	**Symbol Rate $R_{D,\text{E1-Y}}$ (symbols/s)**
B	250
C	No data ('pilot component')

The E1 composite signal is then generated according to Eq. 2.9 below, with the binary signal components $e_{E1\text{-}B}(t)$ and $e_{E1\text{-}C}(t)$. Note that as for E6, both pilot and data components are modulated onto the same carrier component, with a power sharing of 50 percent.

$$s_{E1}(t) = \frac{1}{\sqrt{2}}(e_{E1-B}(t)(\alpha\, sc_{E1-B,a}(t) + \beta\, sc_{E1-B,b}(t)) - e_{E1-C}(t)(\alpha\, sc_{E1-C,a}(t) - \beta\, sc_{E1-C,b}(t))) \tag{2.9}$$

2.5.1. Logic Level

The correspondence between the logic level code bits used to modulate the signal and the signal level is according to the values stated in Table 2.6 [1]. This corresponds to BPSK symbol mapping.

Table 2.6: *Logic to Signal Level Assignment.*

Logic Level	**Signal Level**
1	-1.0
0	+1.0

The edge of each data symbol coincides with the edge of a code chip. A periodic spreading code coincides with the start of a data symbol. The edge of each secondary code chip coincides with the edge of a primary code chip. Primary code start coincides with the start of a secondary code chip [1].

2.5.2. Received Power Levels on Ground

The Galileo satellites will provide Galileo E5, E6 and E1 signals strength in order to meet the minimum levels specified in Table 2.7. The minimum received power on ground is measured at the output of an ideally matched Right-Hand Circular Polarization (RHCP) 0 dBi polarized user receiving antenna when satellite elevation angle is higher than 10 degrees. For a 5 degree user elevation angle, the user minimum received power will be typically 0.25 dB lower than what specified in Table 2.7 [1].

Table 2.7: *Logic to Signal Level Assignment.*

Signal	Signal Component	Total Received Minimum Power (dBW)
E5	E5a	-155
	E5b	-155
E6	E6 CS (components B+C)	-155
E1	E1 OS (components B+C)	-157

Using the same assumptions, the user's maximum received signal power level is not expected to exceed 3 dB above the corresponding minimum received power. For purposes of establishing user receiver dynamic range for receiver design and test, the maximum received signal power level is not expected to exceed 7 dB above the corresponding minimum received power [1].

Chapter 3

Delay-Doppler Acquisition of Galileo Signals

Acquisition is the first step in the digital signal processing section of a GNSS receiver. The process of detecting a specific satellite signal and the coarse propagation time delay and Doppler shift corresponding to a particular satellite-receiver link is called acquisition. Its purpose is to determine visible satellites and to provide estimates of code phase and Doppler frequency of the satellite signals. A GNSS receiver has to detect the presence of a satellite signal in order to be able to track and decode the information which enables position, velocity and time computation. The acquisition stage is followed by the tracking stage, where the synchronization with higher accuracy is performed and maintained. This chapter discusses the concepts of signal acquisition in a GNSS receiver.

3.1 Signal Acquisition

The purpose of acquisition is to determine visible satellites and to produce coarse estimates of carrier frequency and code phase of the satellite signals. Each satellite is distinguished by a unique pseudorandom noise sequence. The basic idea of the search process is to know the code phase of the received signal in order to generate a local PRN code [24]. It is generated to de-spread the signal (i.e. remove the code). The incoming code can be removed successfully only when there is an alignment between the received signal and the local generated code. Besides code delay estimation, the Doppler frequency shift has to be determined as well, since its value varies over time due to the continuous motion of the satellite (it may also be due to the motion of the receiver). In the worst case, the Doppler frequency can deviate up to 10 KHz. It is

important to know the frequency of the incoming signal in order to be able to generate a local carrier signal which is used to remove the carrier from the incoming signal [16].

Figure 3.1 depicts a simplified block diagram of code acquisition stage. First, the received signal is correlated with the locally generated PRN code, followed by coherent integration over Nc chips (coherent integration period or coherent integration length) where I- and Q-branches of the complex signals are Integrated and Dumped (I&D) to form the correlation output. I&D-block is also used to perform coherent integration which acts as a low pass filter. The I&D-block removes the higher frequency components from the signal. Coherent integration is further followed by non-coherent integration over Nnc blocks (non-coherent integration length). Non-coherent integration is basically used to decrease the noise floor and also because the coherent integration time Nc could be limited by channel fading, Doppler effects [27] and by the instability of the oscillator clocks.

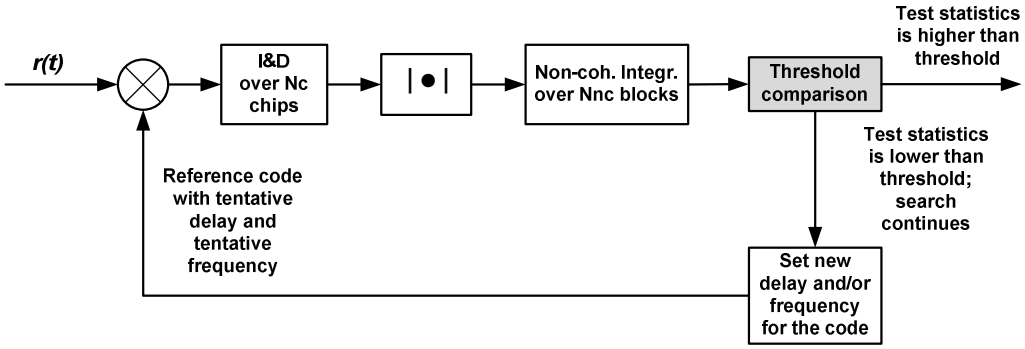

Figure 3.1: *Simplified Block Diagram of Code Acquisition Stage.*

3.1.1. Correlation

The tentative time-frequency bins are tested and the signal is detected via cross-correlation and comparison with a threshold. This means that the received signal is correlated with the reference code with different code phases and frequencies, and then the resulting values are combined in order to achieve a two-dimensional correlation output for the whole window. A correlation peak will be present only in the correct code-frequency bin. Based on the correlation outputs, we can determine whether we are in a correct search window (or bin), i.e., if signal is present, or whether we are in an incorrect search window or bin, i.e., signal is absent. In an ideal case, if the auto- and

cross correlation properties of the codes are perfect and in the absence of any types of noise, the autocorrelation function would be modeled by a pure Dirac pulse at the correct delay and would have zero values elsewhere. However, there are always some signal interference and noise present, which affect the correlation outputs of the received signal and reference code. The reference signal for a CBOC-modulated signal can be either CBOC-modulated or SinBOC(1,1)-modulated code. Hence, both approaches have been considered under the scope of this thesis work.

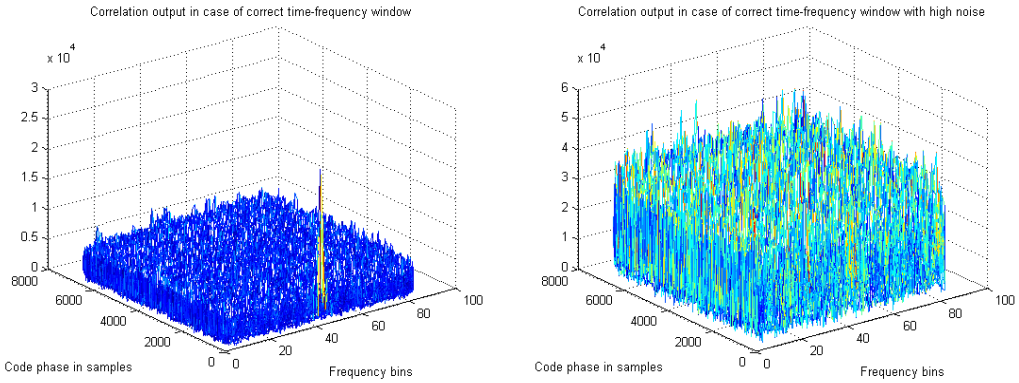

Figure 3.2: *An example of correlation outputs for two time-frequency windows: A correct window with low noise (left) and a correct window with high noise (right). The coherent integration length Nc = 4 ms.*

Figure 3.2 depicts time-frequency mesh of correlation output for correct window with low noise for $C/N_0 = 50$ dB-Hz (i.e. signal is present) and for correct window with $C/N_0 = 35$ dB-Hz, (i.e. signal is still present) but with high noise. This plot is obtained using CBOC('+/-') modulation. The correlation output is compared with the specified detection threshold to see if the signal is present or not. It can be observed in the plots that in very noisy scenarios (e.g., in indoor environment), the signal is not strong enough, thus many correlation peaks are present in the correlation output, which makes the acquisition process quite challenging.

3.1.2. Search Space

The signal acquisition process is a two-dimensional search in time (code phase) and frequency (Doppler offset) which requires the replication of both code and the carrier of the incoming signal in order to detect the satellite [25]. The search space for code delay is typically equal to the length of the code which is 4092 chips in the case of Galileo

E1-B and E1-C signals. The search interval for the Doppler frequency domain can be several KHz [26]. In the acquisition stage, it is preferable to have some a-priori information about Doppler frequency (e.g., assisted acquisition) because it would help to reduce the search time.

Figure 3.3 depicts a two dimensional C/A code search pattern. In the search process, all possible code delay and frequency combinations are examined with some pre-defined search steps. The two-dimensional search pattern consists of discrete search cells with each cell representing one code bin (or a time bin) and one carrier Doppler bin (or a frequency bin). The size of one code bin is typically 0.5 chips for GPS signals [2] and 0.175 chips for CBOC and SinBOC(1,1) signals because most of the signals energy is found within half of the width of the main lobe of auto-correlation function. The combination of one code bin and one Doppler bin makes a test cell or a time-frequency bin. The whole time frequency-uncertainty region can be divided into several search windows and each window can be divided into several time-frequency bins. In Figure 3.3, Δf_{bin} represents one frequency bin length and Δt_{bin} represents one time bin length [2].

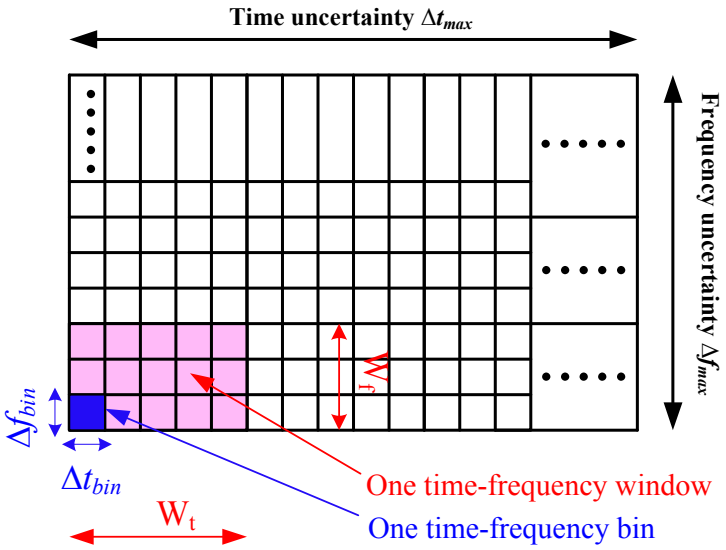

Figure 3.3: *Two dimensional GNSS code search pattern.*

3.1.3. Search Strategy

In the search pattern, the search windows are examined to see whether the time-frequency estimate is correct or not. The search process is started from one search window, with a certain tentative Doppler frequency and a certain tentative code delay. All delays and frequencies, which correspond to the size of the search window at issue, are searched through with the pre-defined search steps. If the window is decided to be dismissed, the search process continues to the next search window, and the same procedure is continued, until the correct window and the correct delay-frequency combination are found [1][24].

3.1.3.1 Serial Search

In serial search, the search window consists of one bin and the delay shift is changed by steps of the time-bin length Δt_{bin}. Thus, all bins are searched one by one in a serial manner and only one search detector is needed for the acquisition structure. The received signal is complex; therefore, one search detector contains two real correlators, one for the real part (I-branch) and other for the complex part (Q-branch) [23].

Serial search approach goes in a way that, it tests one time-frequency bins at a time which, in the end, leads to a very time consuming process if the uncertainty regions are large. For this reason, this method is mostly used if there is some assistance information available about the correct Doppler and code delay [24]. The serial search is rather time consuming because it performs two different sweeps: a frequency sweep over all possible carrier frequencies and a code phase sweep over all different code phase. This exhausting search routine also tends to be the main weakness of the serial search algorithms [28].

3.1.3.2 Fully Parallel Search

This method of acquisition parallelizes the search for one of the parameters (i.e. code-delay or Doppler bin). In fully parallel search strategy, there is only one window in the search space, i.e., the window size is equal to the code-frequency uncertainty. In parallel search strategy, code-frequency bins are examined concurrently. Although it reduces the acquisition time, the complexity increases, since more correlators are needed [29]. This

is the reason why such approach is preferable in software defined receivers. Parallel search strategy has been used in the Simulink model for this thesis.

3.1.3.3 Hybrid Search

As described above, serial search requires only one complex correlator (i.e., two real correlators), which makes the implementation of the algorithm quite simple. However, acquisition time can be too high if the search space is large. With fully parallel search faster acquisition can be achieved, but at the same time complexity increases as more correlators are needed. A hybrid search is a tradeoff between the fully parallel and serial searches strategies and it allows achieving a proper balance between the acquisition speed and the hardware complexity. In hybrid search strategy, the number of bins per window is still limited by the feasible numbers of correlators [23][29][31].

3.1.4. Detection Threshold

The choice of a suitable detection threshold has a great importance in the acquisition process. Figure 3.4 illustrates the Probability Density Function (PDF) of a detection stage. It can be easily noticed in the Figure 3.4 that if the detection threshold is set too low, the probability of detection (i.e., P_d) increases, but on the other hand, the probability of false alarm (i.e., P_{fa}) increases as well. In the same way, if the detection threshold is set too high, P_{fa} decreases but at the same time P_d decreases as well. A brief discussion about selecting a suitable detection threshold can be found, for example, in [23].

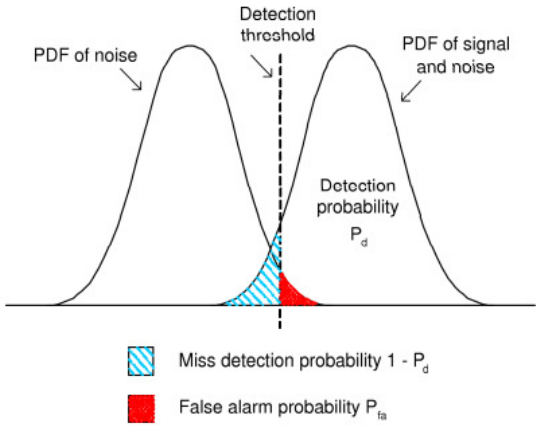

Figure 3.4: *PDFs for correct and incorrect windows.*

3.2 Detection and False Alarm Probabilities

In the detection stage, the test statistics are computed based on the correlation output for each search window, and then this statistics are compared to pre-defined threshold 'γ' in order to decide whether the signal is present or not. The test statistics can be formed in the following ways:

- as the global maximum of the correlation output in one search window [26][37].
- as the ratio between the global maximum and the next local maximum [38][39].

If the value of the test statistics is higher than the specified threshold, it means that the signal is detected and an estimate for code-phase and frequency is achieved. If the peak is not detected, the process continues in the next search window.

The detection probability in this thesis is defined as the probability of signal being detected correctly if the maximum code phase error is within 0.35 chips and maximum frequency error is within 125 Hz. In the same way, a false alarm situation occurs when a delay and/or frequency estimate is wrong (i.e. absolute error in code higher than 0.35 chips and absolute error in frequency higher than 125 Hz) but still the test statistics is higher than the threshold. In this case, the signal is declared present in an incorrect window. The probability of a false alarm case is denoted as P_{fa}. It may also be the case that signal is present but not detected. This may happens if the threshold is set too high or the environment is so noisy that the signal is lost in the background noise [23][26]. This is a miss detection situation.

3.3 Standard Methods of Acquisition

In Galileo system, the proposed lengths for the spreading codes are higher than in the GPS system, e.g., 4092 chips for E1-B and E1-C signals [14]. As described earlier, signals acquisition involves a two-dimensional search in time and frequency domain. Thus, the acquisition of Galileo signals is more time consuming due to the larger uncertainty regions. In the search for fast and efficient acquisition methods, several search algorithms have been developed. The following sections describe the theory behind three standard methods of acquisition to demonstrate the possibility of implementing an efficient method in a software receiver.

3.3.1. Ambiguous Acquisition

Auto-correlation functions of BOC and MBOC modulation schemes bring new challenges in acquisition process. BOC- and MBOC- modulated signals have narrower main lobes in their ACFs, which allow better accuracy in the tracking stage. On the other hand, additional peaks appear within ± 1 chip interval around the maximum peak, which make the ACF to become ambiguous. These challenges can be solved to a certain extent by using unambiguous acquisition methods such as those mentioned in the previous section. However, such methods are out of the scope of this thesis, therefore they will not be considered.

Figure 3.5 shows the envelope of the normalized ACFs of SinBOC(1,1) and CBOC('+/-') modulations where additional peaks can be seen; these peaks will cause more challenges to the acquisition process. In order to detect the main lobe of the ACF, the step 'Δt_{bin}' for searching the time bins in the acquisition process should be sufficiently small [32]. The process becomes more challenging when the reception is performed in indoor environment, where CNR is very low.

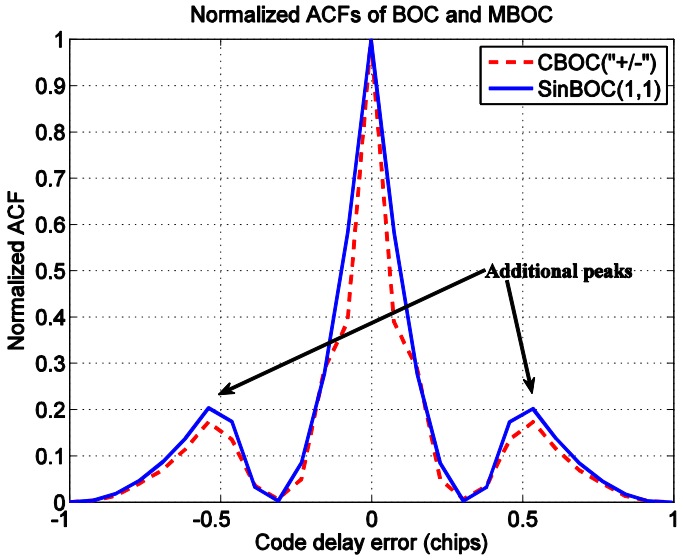

Figure 3.5: *Normalized ACFs of SinBOC(1,1) and CBOC('+/-')ambiguous acquisition.*

3.3.2. Unambiguous Acquisition

Several algorithms have been proposed in order to deal with the ambiguities of the envelope of the ACF of BOC or MBOC modulation and to increase the step for the

time-bin in the acquisition process which helps to decrease the acquisition time. These techniques are: 'BPSK- like techniques', proposed by Martin, Heiries et al. [33][34], the sideband (SB) techniques' proposed by Betz, Fishman et al. [16][21][22] and Unsuppressed Adjacent Lobes (UAL) method [35]. These techniques are based on the idea that the BOC- or MBOC-modulated signal can be seen as a superposition of two BPSK modulated signals, located at negative and positive subcarrier frequencies. All these techniques can make use of the single- or the dual- side band signal approach [36]. These algorithms are not addressed in this thesis because of the fact that FFT-based acquisition is used here, with step equal to 1/fs, , where fs is the sampling frequency and is equal to 13 MHz, and therefore, a sufficiently small step was used to justify the choice of ambiguous methods.

Chapter 4

Simulink Model for Galileo Signal Acquisition

The complete Galileo Simulink model has been developed at Tampere University of Technology, Finland. In the basic Simulink model, the whole E1 chain is implemented, including the E1 transmitter block, the multi-path channel, the acquisition block and the tracking unit block. The E1 signal is composed of E1-B and E1-C channels, data signal is carried by E1-B channel and E1-C carries the pilot channel. Both E1-B and E1-C channels are tracked in the Simulink model. There are 2 receiver options: one which uses a reference SinBOC(1,1) modulated code for both E1-B and E1-C, another one which uses a reference CBOC(+)-modulated code for E1-B and a reference CBOC(-)-modulated code for E1-C. A new acquisition model based on CBOC reference signal has been built by the author (basic model included only the SinBOC(1,1) acquisition). Modification of the acquisition block has been done in order to allow for variable time-bin steps. In the original model, a fixed time-bin step was used in the acquisition unit. The author extended the original model to variable time-bin steps. Additionally, the implementation of switching architecture is done, where E1 and E5 transmitters alternate periodically and the reception is done based on E1 signal only. A study was carried out in order to investigate the impact of detection probability using different acquisition thresholds. The effects of front-end bandwidth on the performance of signal in terms of detection probability are also presented here. These issues are described in this chapter and they constitute the main research results for this thesis.

4.1 Description of the Simulink Model

The Simulink model consists of a transmitter block, a channel block, an acquisition block and a tracking block. Figure 4.1 illustrates the block diagram of the whole E1 chain. Next section describes the details about the individual blocks of E1 chain model.

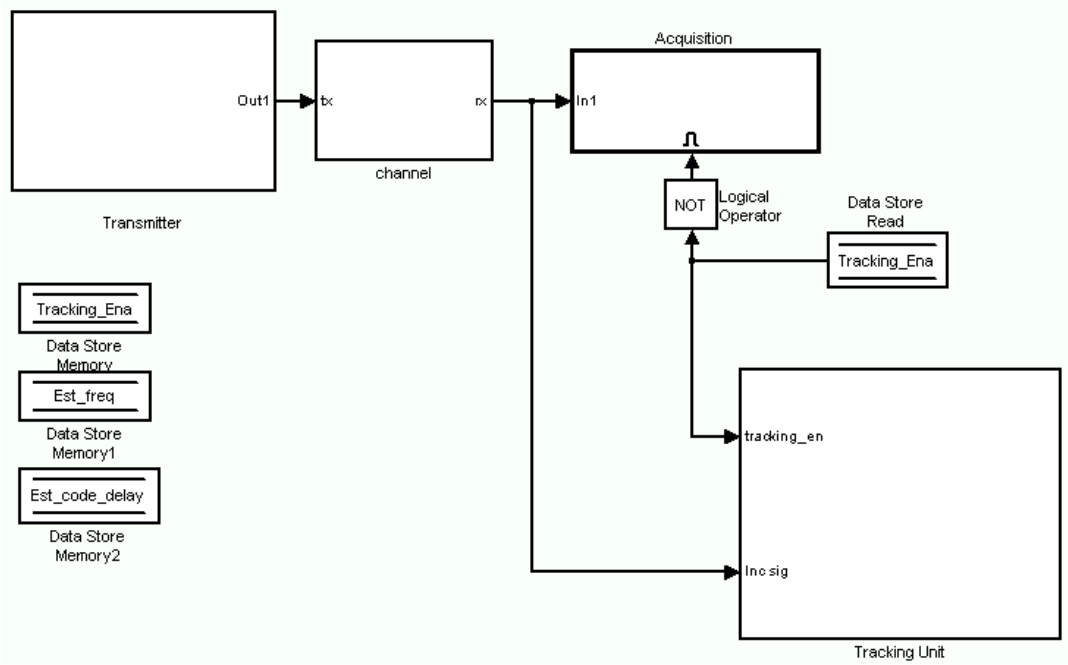

Figure 4.1: *A snapshot of whole E1 Chain Simulink model.*

4.1.1. Transmitter Block

The E1 transmitter block is implemented based on CBOC modulation, which is in accordance with the latest Galileo OS ICD [1]. In the block, E1-B and E1-C channels, in which the OS signals are carried on, are modeled according to Eq. 2.9.

Figure 4.2 shows the snapshot of the E1 transmitter Simulink block. The code length for the Galileo OS signal is 4092 chips, which is four times higher than the GPS C/A code length. The code epoch length is 4 ms, which means that the codes are not the same from one code symbol to another. Moreover, the spreading factor for this model is considered to be the same as for the C/A GPS signals (i.e. 1023 chips where one code symbol having 1 ms duration) in order to avoid long simulation times. In each frame, $fs*10^{-3}$ samples are included, for example, each frame contains 13,000 samples when

the sampling rate is 13 MHz. Table 4.1 shows some of the input parameters used for this Simulink model.

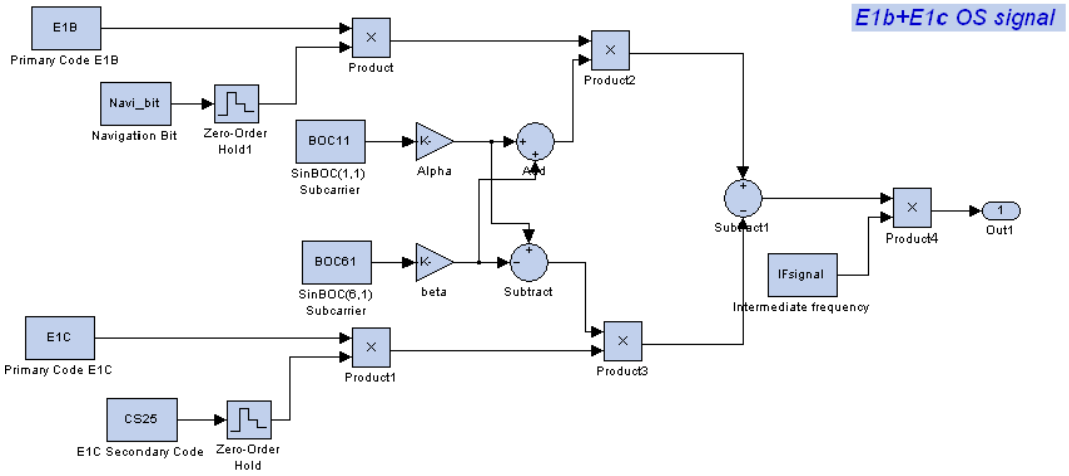

Figure 4.2: *A snapshot of the E1 transmitter Simulink block.*

- In the transmitter block, E1-B is the CBOC('+') modulated signal with navigation data (upper part) and E1-C is the CBOC('-') modulated signal without data (pilot channel). E1 signal is formed as the difference between the two signals above-mentioned (Eq. 4.1).

- In E1-C channel, there is no navigation data, but only a secondary code.

- The sampling frequency *fs* is a variable of the model (currently, it is set to 13 MHz).

Table 4.1: *Input parameters used for Simulink model.*

Variable Name	Description	Unit	Dimension	Typical Value
sv	Satellite index for selecting the corresponding code		1	1~50
fs	Sampling frequency	Hz	1	any value OK
fIF	Intermediate frequency	Hz	1	any value OK
Navi_bit	Navigation bit		≥	1, -1

4.1.2. Channel

In the channel block, only the multi-path signals and complex noise are generated. The basic function of the channel block can be modeled as

$$r_{E1}(t) = \sum_{i=1}^{l} \alpha_i(t) s_{E1}(t - \tau_i) + n(t) \tag{4.1}$$

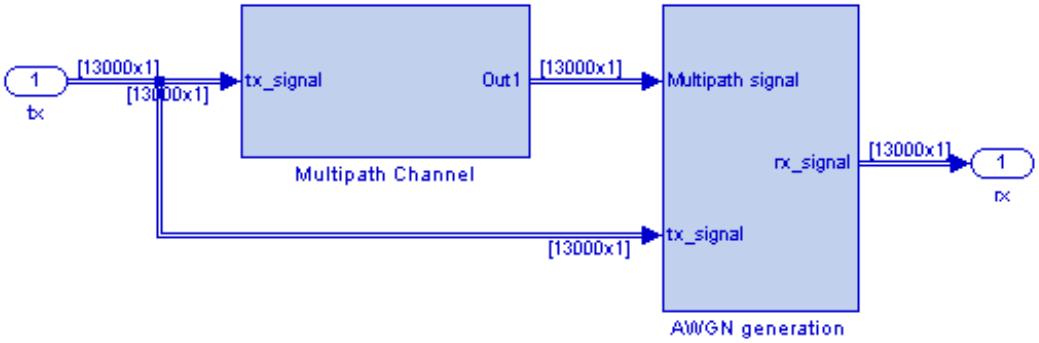

Figure 4.3: *A Snapshot of the channel Simulink block.*

Here $r_{E1}(t)$ is the received E1 signal, which is the output of the channel block; $\alpha_i(t)$ and τ_i are the time-varying path gain with complex value and path delay for *i*-th path; n(t) is the AWGN. Figure 4.3 depicts the block diagram of channel used for this model.

- The path amplitude remains the same within 1 ms, which is the frame duration of the signal in the transmitter and channel. This is because the Doppler spread is usually small.

- Only 'static' channel is used during the reported simulation.

- The whole chain is in Intermediate Frequency (IF). Therefore, the carrier phase is also affected by the path delay. Therefore, for MEE (Mean Error Envelopes) simulation, it is better to use a baseband chain by setting the fIF to be 0 in order to avoid the carrier phase errors.

4.1.3. Acquisition Block

The acquisition unit performs FFT-based correlation. The Fourier transform of the input signal is multiplied with the Fourier transform of the PRN code. The result of the multiplication is transformed into time domain by taking inverse Fourier transform. The absolute value of the output of the inverse Fourier transform represents the correlation between the input and the PRN code. Figure 4.4 shows the block diagram of acquisition block implemented partly using Matlab based S-function.

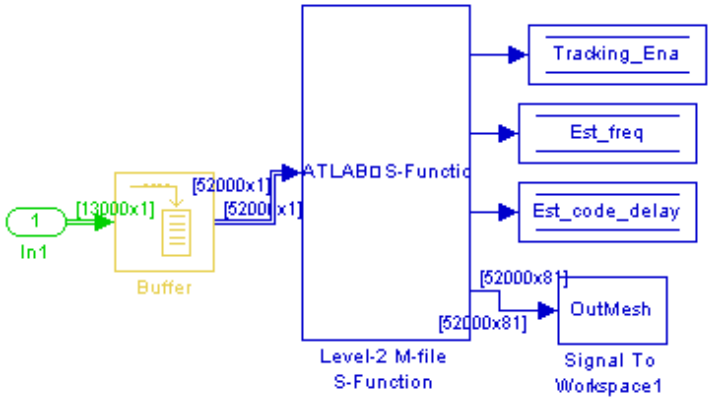

Figure 4.4: *A snapshot of acquisition Simulink block.*

The acquisition detection is implemented according to a Constant False Alarm Rate (CFAR) algorithm explained briefly in [20]. The acquisition is implemented using m-language based S-function. The input and output data and the parameters of this block are listed in table 4.2.

With CFAR algorithm, the decision is made based on the correlation output. Here we use the average of the absolute values of E1-B and E1-C correlation outputs. The acquisition decision variable will be according to the ratio of peaks (which will be explained in the next section), after setting to 0 a neighborhood of a time range between -3 and 3 chips and a frequency range between -500 and 500 Hz. The detection threshold values between 1.27 and 1.3 have been used for simulations.

The output data are stored in the memory, using the Simulink library block ‘Data Store Memory’, i.e. ‘Tracking_Ena’, ‘Est_freq’ and ‘Est_code_delay’. The stored data are read outside the acquisition block, for instance, in the tracking unit. Once the correlation

output is higher than specified threshold, the output parameter 'Tracking_Ena' will enable the tracking part. The estimated frequency and code phase of the signal can be examined by the parameters 'Est_freq' and 'Est_code_delay', respectively. The focus in this thesis is on the acquisition part and therefore tracking will not be discussed in detail.

Table 4.2: *Acquisition unit input and output data and other parameters.*

	Description	**Unit**	**Typical Values**
Input data	Incoming signal of duration 4 ms	Samples	Vector
Output data	Tracking Unit enabling signal	Unitless	Scalar
	Estimated frequency from acquisition	Hz	Scalar
	Estimated code delay from acquisition	Chip	Scalar
Parameters	Sampled E1-B reference signal (the BOC(1,1) or CBOC(+)-modulated E1-B primary code)	Samples	Vector
	Sampled E1-C reference signal (the BOC(1,1) or CBOC(-)-modulated E1-C primary code)	Samples	Vector
	Frequency uncertainty range	Hz	fIF+ (-1000:500:1000)
	Receiver sampling frequency	Hz	fs
	Acquisition detection threshold	Unitless	e.g., (1.3-1.4)

Currently, the coherent integration is 4 milliseconds. Therefore, the frequency uncertainty range is from -5 kHz to + 5 kHz with step of 125 Hz. The frequency uncertainty range can be redefined according to the requirements. The time uncertainty range is equal to 4 ms code epoch; the time-bin step is equal to 1 sample. In the basic block, the time bin step was limited to 1 sample, but the modified block with variable time-bin steps which is the focus of this thesis will be described in Section 4.2.2. We remark that in the original implementation of the acquisition unit, the reference code at the receiver is the SinBOC(1,1)-modulated code. In order to use the CBOC reference receiver as well, the author did modifications to the original model that are explained in Section 4.2.1.

4.1.4. Tracking Block

The tracking block is not addressed here since it is out of the scope of this thesis, but the basic tracking block contains a FLL, a PLL and a code tracking loop based on early-minus-late power discriminator from literature, e.g. the one found in [2]. In the 'Dual channel correlation and discriminator' block, E1-B and E1-C channels are implemented separately.

4.2 Modified Acquisition Block

The main focus of this thesis was to build new blocks and modify the functionality of some existing blocks in the Simulink model i.e. by introducing new acquisition unit with CBOC reference code, implementing a switching architecture model and modifying the time-bin steps in the acquisition. The author also studied the impact of the acquisition threshold on the detection probabilities. In what follows, we briefly explain the modifications which have taken place under the scope of this thesis.

4.2.1. CBOC Based Acquisition Unit

The main modification which was done is the introduction of another acquisition unit in the previous model shown in Figure 4.1 based on CBOC modulated code. The key idea of introducing this block is to study the behavior of CBOC signal in terms of detection probability, mean error and variance which will be explained briefly in Chapter 5.

In the previous model, the reference code at the receiver was the SinBOC(1,1) but now CBOC based reference code has also been implemented which works in the same way as the previous model. This new acquisition unit improves the reception because CBOC-modulated signals have better characteristics, due to a narrower correlation function. CBOC signal structure allows the receivers to obtain high performance in terms of multi-path rejection and tracking. Here we used the average of absolute of CBOC data and CBOC pilot. Figure 4.5 shows the modified block diagram of acquisition unit. In the model, the data channel is implemented using CBOC('+') modulation scheme according to Eq. 2.6. In the same way, the pilot channel is implemented according to Eq. 2.7.

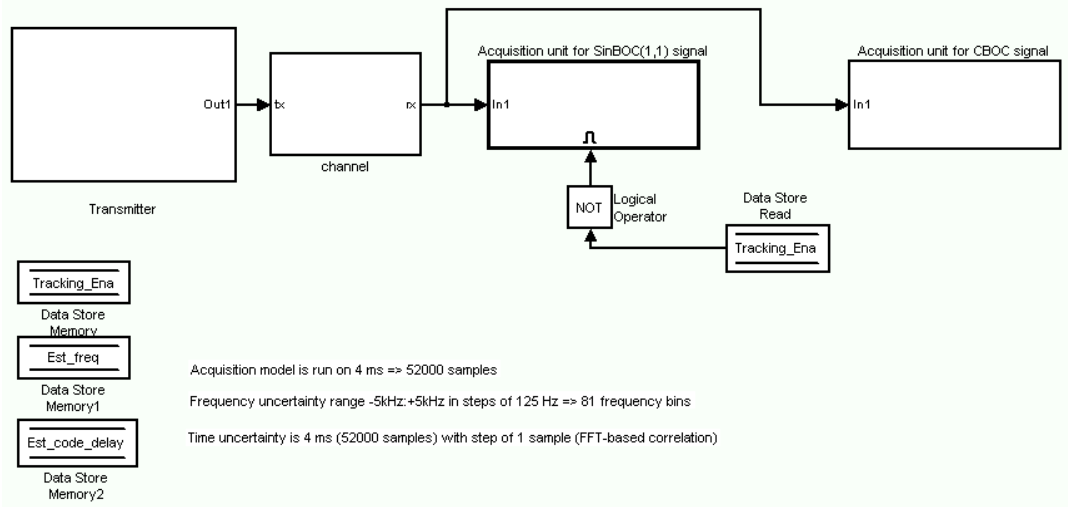

Figure 4.5: *A snapshot of modified acquisition Simulink block*

4.2.2. Variable time-bin Step

As explained in previous chapters the Galileo spreading code lengths are much longer than the traditional GPS C/A code. The dimension of the search space for Galileo signals increases with the code length. For the new codes, a traditional sequential acquisition algorithm is not practical because it results in unacceptable acquisition times. Parallel search strategy has been used in the Simulink model for this thesis. In the previous model, the time uncertainty range is equal to 4 ms code epoch; the time-bin step 'Δt_{bin}' is equal to 1 BOC or CBOC sample, 1 sample time-bin step results in 52 000 samples all together which indeed spend a significant amount of time in baseband processing for acquisition.

From the point of view of real-life applications, acquisition process should be fast enough to detect the signal. Based on these observations, acquisition block has been modified for steps higher than 1 BOC/CBOC sample. The effect of variable time-bin step is clearly visible from Figure 4.6. Further discussion about the performance of the model based on this modification will be presented in the next section.

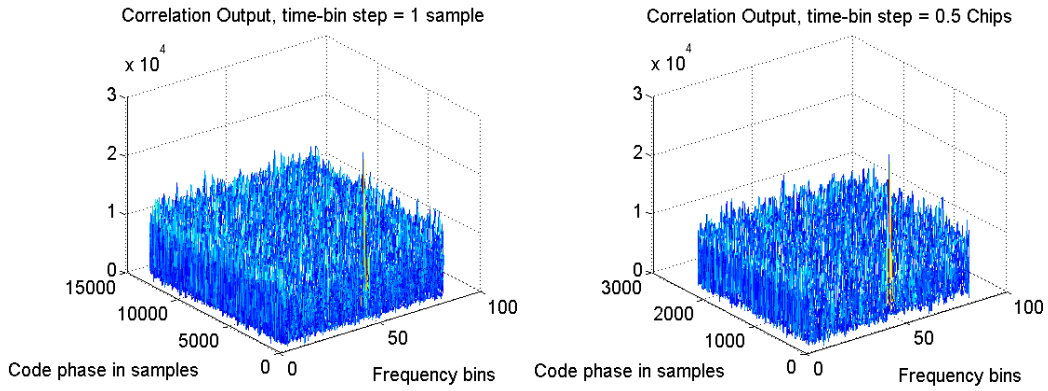

Figure 4.6: *A correct time-frequency window with time-bin step = 1 sample (left) and a correct window with time-bin step = 0.5 chips (right).*

4.2.3. Choice of the time-bin Size

The acquisition process becomes more complex due to ambiguities (i.e. additional peaks within ± 1 chip interval around the main lobe) present in the envelope of the ACF. The steps 'Δt_{bin}' for searching the time axis have to be chosen quite carefully to avoid the ambiguities and to be able to detect the signal carefully. Thus, the acquisition becomes more computationally expensive, the computational load being inversely proportional with the time-bin size (or step) 'Δt_{bin}' [35]. Typically, a step of Δt_{bin} = 0.5 chips is used in BPSK modulation (i.e. C/A code for GPS) [2]. The presence of BOC modulation also creates some additional deep fades within ±1 chip from the main peak. For this reason, a time-bin step of 0.5 chips is typically not sufficient and smaller steps need to be used for BOC modulated signals. On the other hand, smaller 'Δt_{bin}' means more time will be consumed while searching for more bins that will increase the mean acquisition time and the complexity of the receiver [42].

A rule of thumb for selecting the step-time bin should be typically half of the width of the main lobe (e.g., 0.5 chips in GPS BPSK-modulated signals, about 0.35 chips in Galileo MBOC/SinBOC(1,1)-modulated signals) [36]. Figure 3.5 shows the autocorrelation function of SinBOC(1,1) and CBOC('+/-'). It can be noticed that, one fourth of the width of the main lobes of ACF envelope for SinBOC(1,1) and CBOC('+/-') is around 0.175 chips, which needs to be set as a step 'Δt_{bin}' for time-bin window for correct acquisition.

4.2.4. Switching Architecture Studies

A switching architecture has been introduced into the Simulink model of E1 chain. The transmitter operates at dual frequency i.e. E1 and E5 bands, which were down converted to same intermediate frequency. The basic idea for introducing this feature is to study the behavior of jointly transmitted signals in terms of detection probability. Figure 4.7 depicts the block diagram of switched transmitter model. In the transmitter model, E1 and E5 transmitters have been combined through a switch. In other words, only one front-end is used for receiving both E1 and E5 signals. The benefit of such architecture is that the power consumption is lower, which would be an advantage in dual frequency in the future. That is why this section addresses the issue of performance deterioration in baseband if such a switching architecture is employed.

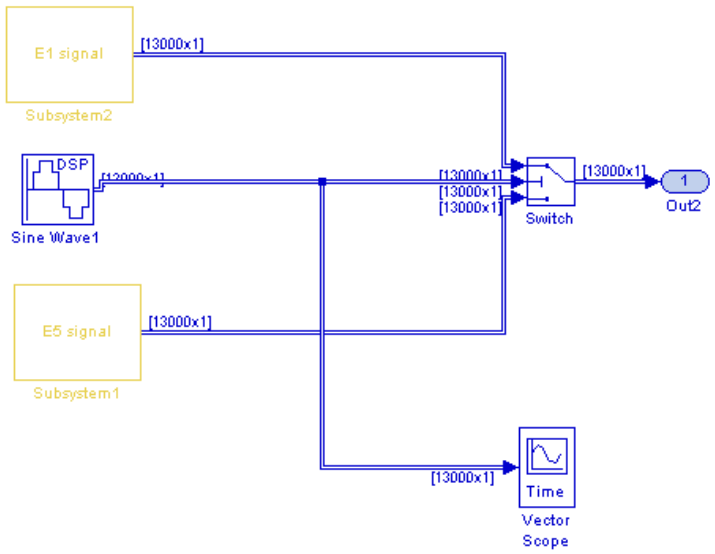

Figure 4.7: *A snapshot of switched transmitter model.*

The Switch block comprises of three inputs. The Switch block passes through the first input or the third input based on the value of the second input. The first and third inputs are called data inputs. The second input is called the control input. A Sine wave block is attached with the control input. Control signal is set to zero. Once the control input is higher than the specified threshold, E1 signal will be transmitted, otherwise E5 signal will be transmitted through the transmitter. A set of different switching time between E1 and E5 transmitters have been set to see how they affect the acquisition in terms of

detection probability. Acquisition model is not employed with E5 reference code, it is still correlating with BOC(1,1) and CBOC signals.

Figure 4.8 shows the simple waveform of switching time between E1 and E5 transmitter. The upper plot of Figure 4.8 shows the sinusoidal waveform used for switching between E1 and E5 transmitter. Here switching time is 2 ms. From the bottom plot, we observe that E1 signal is transmitted for the first 2 ms duration and afterwards, E5 signal is transmitted which is all zero for the simplicity of the model and in order to find out the maximum achievable performance of a switching architecture. This switching architecture has also been studied in the tracking stage in [44]. The simulation results are shown in Chapter 5.

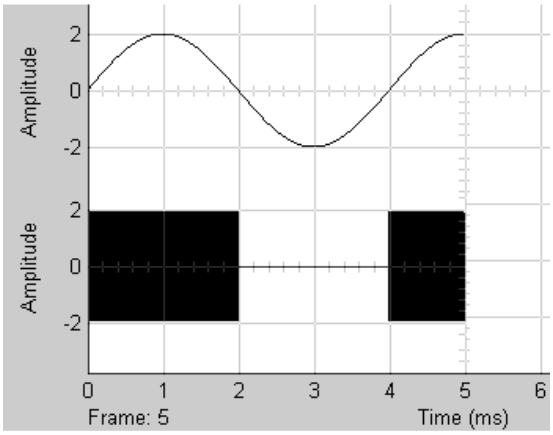

Figure 4.8: *Switching interval between transmitters.*

Figure 4.9 shows the plots of autocorrelation function of joint CBOC signals with different switching time interval (CBOC reference receiver is used here). The effect of different switching intervals on the shape of ACF of CBOC signal is clearly visible e.g. when switching time is less than 2 ms, more than one autocorrelation shape is present due to the fact that E1 transmitter is transmitting the signal more than once. The time 'T' mentioned in each graph is the total period of the sine wave as shown in Figure 4.8 and the switching of the transmitter occurs at half cycle of each time period.

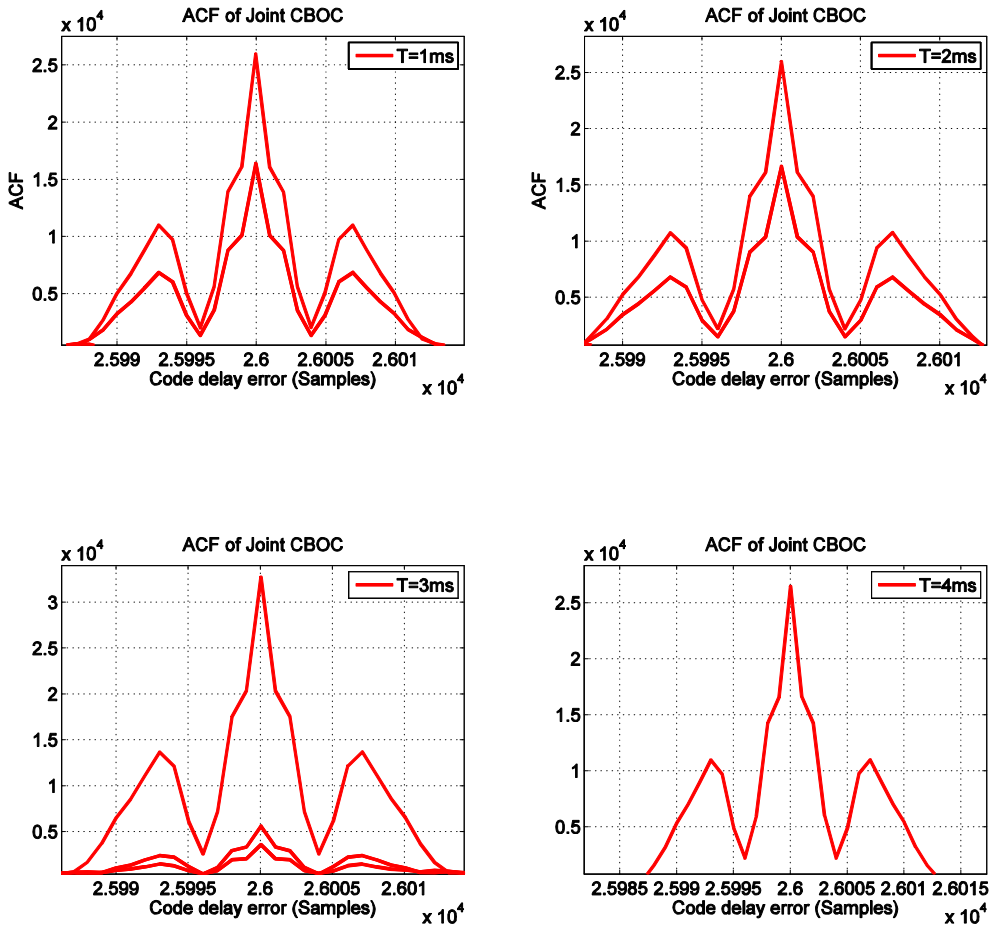

Figure 4.9: *ACFs of joint CBOC signal with different switching interval.*

Chapter 5

Simulink-Based Simulation Results

This chapter presents the simulation based results achieved from the acquisition unit. It starts by presenting the results for detection probability, mean error and variance for the processing of Galileo E1 signal with reference CBOC and reference SinBOC(1,1) receivers, respectively. The results are shown for both single- and multi-path, and for static channels with AWGN. Further plots deal with the comparison of data, pilot and joint data-pilot channel in terms of detection probability, mean error and variance. Additionally, we present the results related to the choice of the weighting factor when combining data and pilot channel, effect of time-bin step on detection probability, effect of limited front-end bandwidth on detection probability. Last section describes the impact of choosing different detection thresholds in terms of detection probability for CBOC reference receiver and also the results based on switching architecture.

5.1 Performance Measures in Simulation

As mentioned in Chapter 4, CBOC unit for acquisition has been introduced in the Simulink model by the author. The main purpose of introducing this block is to make comparison between the BOC and CBOC signals in terms of detection probability. E1 chain model has been simulated according to the following parameters: acquisition unit running time = 5 s, time-bin step in the acquisition Δt_{bin} = 1 sample, multi-path delay spacing is 0.35 chips and the amplitude of the second path is 3 dB lower than the first one. The statistics were computed for 5 s of simulation for each Carrier to Noise Ratio (CNR or C/N0) value. The acquisition threshold is set to 1.27 for both reference BOC and reference CBOC acquisition. All the results computed in this chapter are for infinite bandwidth (or no front-end filter at the receiver).

A test statistic is computed based on the values of code delay error which is calculated by subtracting the true delay from estimated delay, and then this test statistic is compared to a certain threshold in order to plot the detection probability. The code delay error is compared with the threshold equal to 0.175 chips which is one-fourth of the width of the main lobes of ACF envelope of CBOC. The detection probability (P_d) is computed as follows:

$$P_d = prob(Z > \gamma \ \& \ |Delta\ error| < thr\_error) \tag{5.1}$$

Where "| |" means absolute value and "&" means AND operator, 'Z' is the decision statistic, here the correlation output, 'γ' is the decision threshold, here 1.27, 'Delta error' is the delay error in chips, and 'thr_error' is the maximum delay error used as threshold (e.g., 0.175 chips).

The mean error values are expressed in chips and they are computed as:

$$\Delta = \frac{1}{n}\sum_{i=1}^{n}(\widehat{\tau}^{(i)}{}_{LOS} - \tau^{(i)}{}_{LOS}) \tag{5.2}$$

where $\widehat{\tau}^{(i)}{}_{LOS}$ is the estimated LOS delay in chips for i-th observation, $\tau^{(i)}{}_{LOS}$ is the true LOS delay in chips and n is the number of observations (random points) used to compute the statistics.

The variance of the delay error is expressed in units of chips square and is computed as:

$$\sigma^2 = \left(\frac{1}{n}\left(\sum_{i=1}^{n}(\widehat{\tau}^{(i)}{}_{LOS} - \tau^{(i)}{}_{LOS})^2 \right) - \left(\frac{1}{n}\sum_{i=1}^{n}(\widehat{\tau}^{(i)}{}_{LOS} - \tau^{(i)}{}_{LOS}) \right)^2 \right) \tag{5.3}$$

5.2 Detection Probability with Certain Threshold

The results reported in Section 5.3 to 5.8 in this chapter are based on best-case approximation which means that, no matter whether the decision variable is higher or less than the specified threshold, we still output the estimated delay and use it for computing the detection probability. However, it is important to find out how far from

average is the best-case approximation. In this section, we compare the best-case approximation (i.e., no thresholding) with the average detection probability curves for a threshold equal to 1.27. Only the points which are higher than threshold are considered in the statistics. Figure 5.1(a) shows the comparison between the two cases in terms of detection probability for multi-path channel with SinBOC(1,1) and CBOC reference codes, respectively.

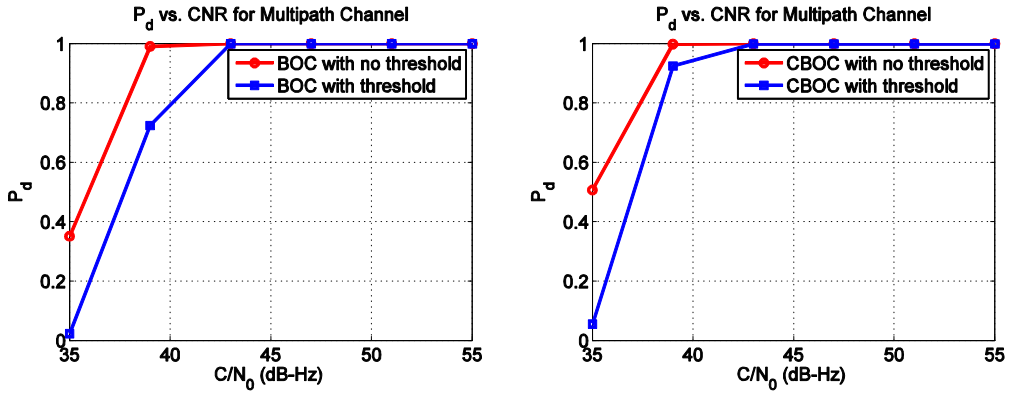

Figure 5.1(a): *P_d versus C/N0 in multi-path channel for SinBOC(1,1) (left) and CBOC reference code (right).*

It can be observed from the plots that best-case is indeed the best in terms of detection probability, it has 2.2 dB and 0.65 dB better detection probabilities with SinBOC(1,1) and CBOC reference code, respectively at P_d = 0.8. On the other hand, it also has an increased false alarm probability which can be observed from Figure 5.1(b).

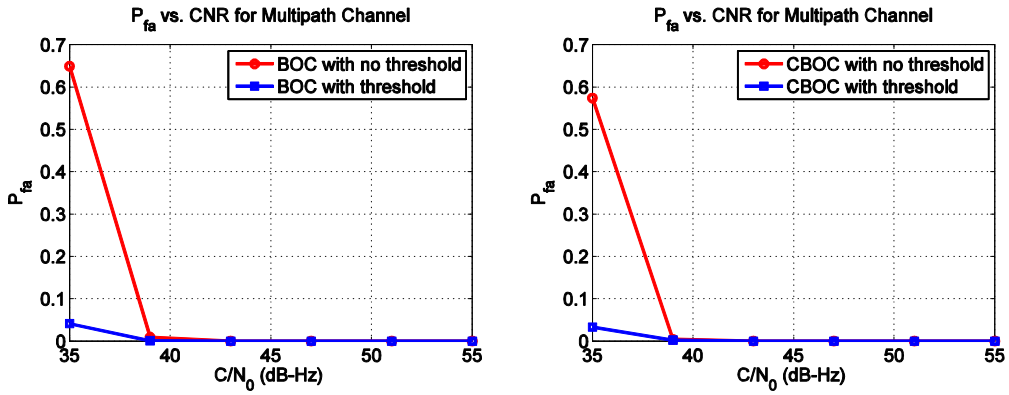

Figure 5.1(b): *P_{fa} versus C/N0 in multi-path channel for SinBOC(1,1) (left) and CBOC reference code (right).*

In what follows, we use the best-case approximation for the simplicity of the calculation. From real receiver's point of view, it is not feasible to use the best-case approximation.

Detection probability is computed using different code delay error thresholds, ranging from 0.15 chips to 1 chip but there is not any significant difference in the performance. In most of the literature, test statistics are computed within 1 chip but we have used 0.175 chips throughout the simulation. The reason is that, for GPS signal, 1 chip represents half of the width of the main lobe. In CBOC case, half of the width of the main correlation lobe is 0.35 chips. If we want to acquire the signal with even higher accuracy than half of the width of the main correlation lobe, it makes sense to use a threshold of 0.175 chips (i.e., if the delay error coming from the acquisition stage is higher, in absolute value, than 0.175 chips then we consider that the signal has not been detected correctly).

5.3 Comparison Between SinBOC(1,1) and CBOC Reference Receiver

Figure 5.2 compares the detection probability, mean absolute error and variance of BOC and CBOC reference receivers. The simulations were carried out in single-path scenario and static channel was considered here. It can be concluded from the figure that at low C/N0 levels, the detection probability of CBOC is better than SinBOC(1,1). As the C/N0 value increases, detection probability also increases. CBOC modulation gives 0.1 dB better detection probability compared to SinBOC(1,1) at P_d = 0.9. As explained already in Chapter 2 MBOC has better power spectral density than SinBOC(1,1). This is mainly due to a higher transition rate (the number of phase transitions per unit time) brought by the BOC(6,1) on top of the BOC(1,1). The contribution of the BOC(6,1) subcarrier brings in an increased amount of power on higher frequencies, which leads to signals with narrower correlation functions and therefore yielding better performance at the receiver level.

Figure 5.3 depict the plots of detection probability, mean error and variance for SinBOC(1,1) and CBOC reference receiver for multi-path channel. First path delay is 0 chips and the second path delay is 0.35 chips. It can be noticed from the figure that at low C/N0 levels, the detection probability of CBOC is better than SinBOC(1,1). CBOC

has 0.15 dB better performance than SinBOC(1,1) at P_d = 0.9. Mean error and variance are converging to zero for both SinBOC(1,1) and CBOC signals but these errors are less for CBOC modulation. In other words, we can say that CBOC has slightly better detection probability in multi-path scenarios as well, but the difference in performance is not higher than 0.15 dB.

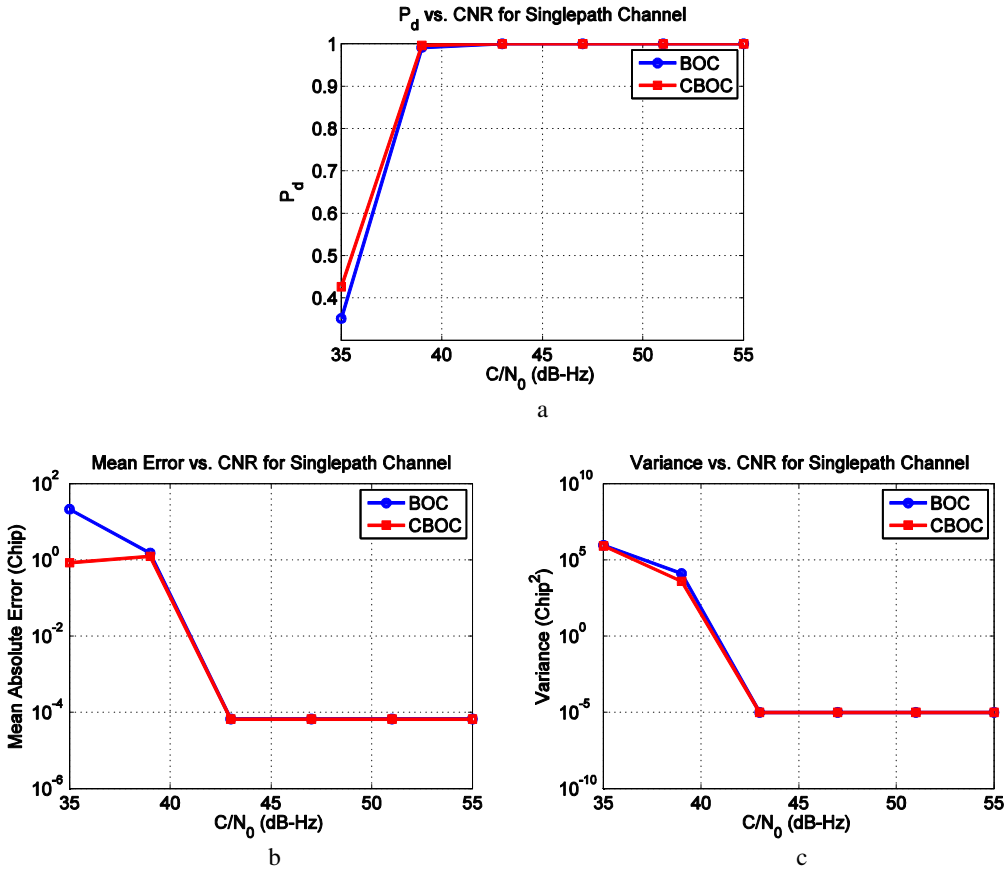

Figure 5.2: *(a) P_d (b) Mean Absolute Error (c) Variance versus C/N0 for single-path channel profile.*

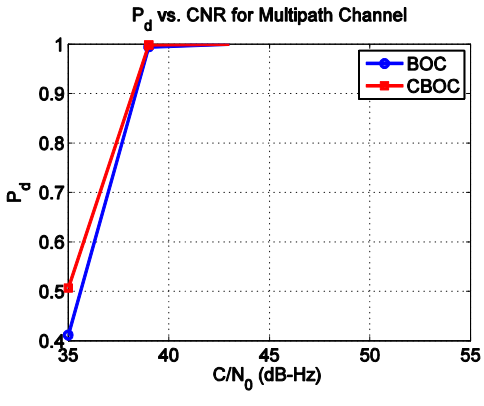

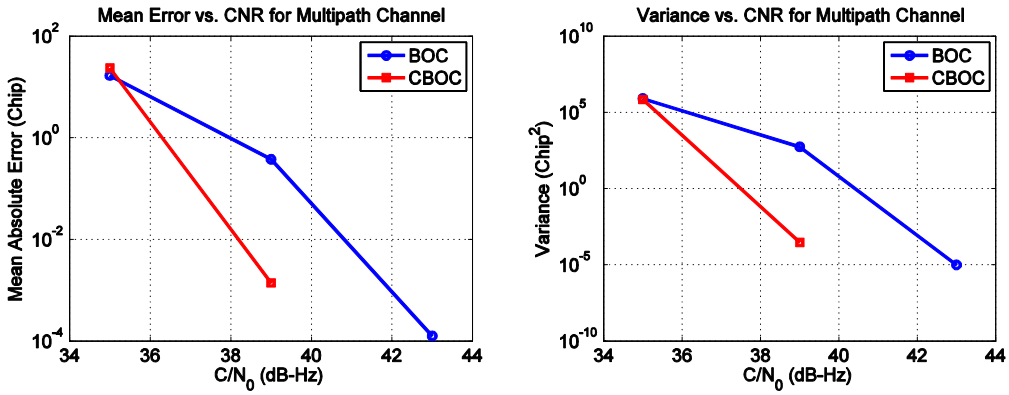

Figure 5.3: *(a) P_d (b) Mean Absolute Error (c) Variance versus C/N0 for multi-path channel profile.*

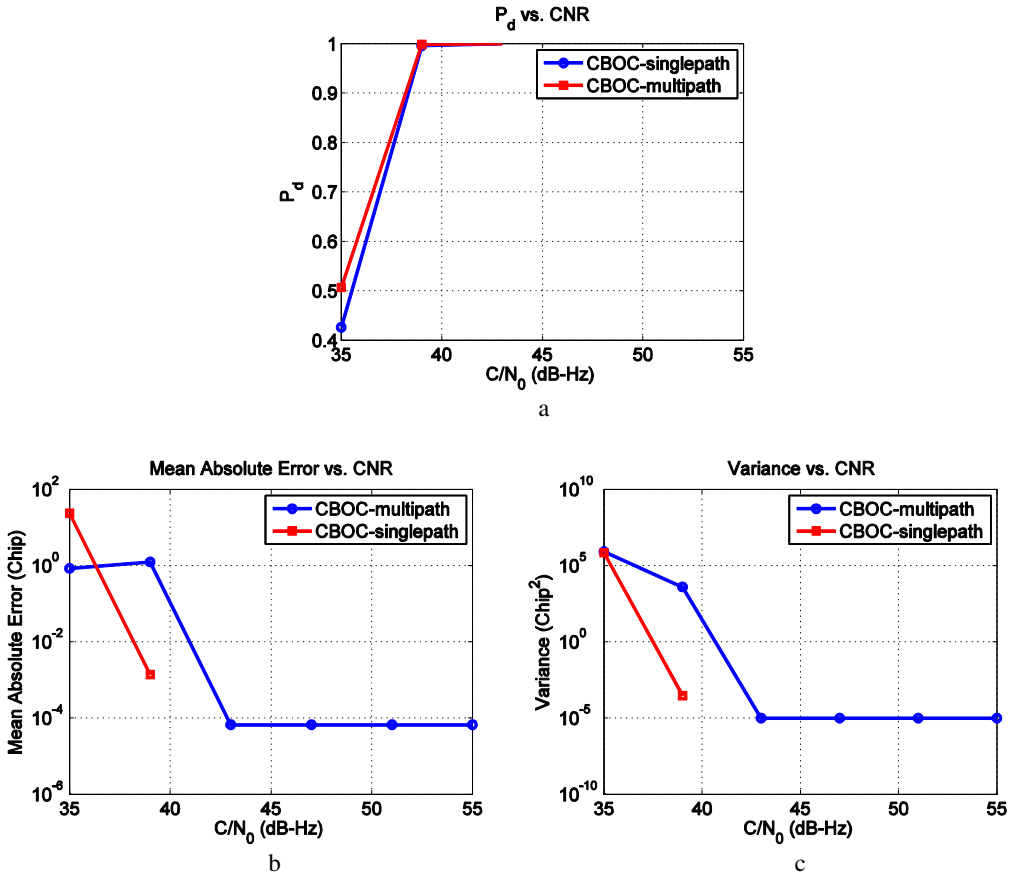

Figure 5.4: *(a) P_d (b) Mean Absolute Error (c) Variance versus C/N0 for single and multi-path channel profile.*

Figure 5.4 depicts the plots of detection probability, mean error and variance of CBOC reference receiver for single-path and multi-path channel profiles. The idea is to compare the performance of CBOC signal in single-path and multi-path channel profiles. It can be seen from Figure 5.4(a) that CBOC reference receiver gives 0.2 dB better performance in single-path channel as compared to multi-path channel at $P_d = 0.8$. It also has less mean and variance error in single-path channel.

5.4 Data-Pilot Combinations for BOC Reference Receiver

The acquisition block has also been modified in order to allow the use of individual channels, i.e. data-only or pilot-only. Comparison among the three different cases (i.e. data-only, pilot-only and non-coherent combining of data and pilot channel) has been made and plots are available for single and multi-path channel profiles. In this non-coherent combining, received signal is correlated individually with the data and pilot local replicas. The correlation outputs are then summed and afterwards, the mean is taken non-coherently over these correlation outputs. It can be easily observed by the plots presented in next sections that non-coherent combining gives more reliable signal detection. BOC reference receiver was used here for the acquisition stage.

We used three different approaches to acquire signal i.e. data-only channel, pilot-only channel and joint data and pilot channel. Considering individual channel to acquire the signal will result in losing half of the useful signal power which degrades the detection probability. Joint data and pilot channel allows recovering of all the available signal power to be used for processing which ultimately improves the signal acquisition and provides better detection probability [4] which can be observed from the Figure 5.5 and 5.6.

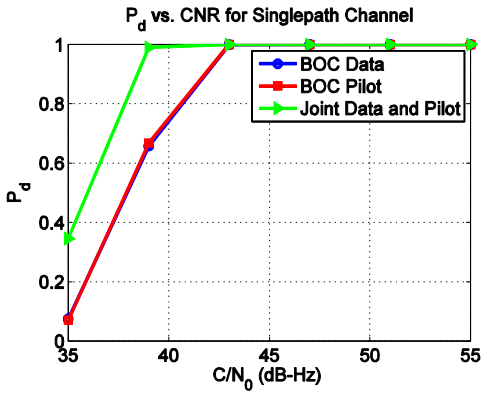

a

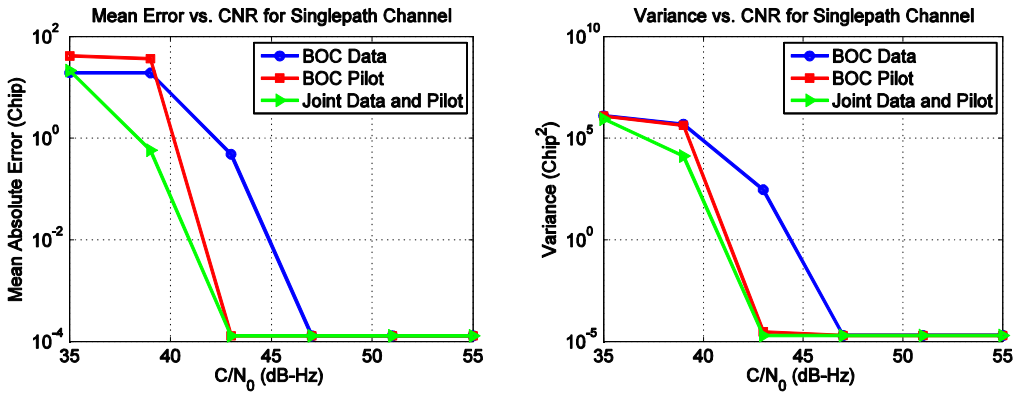

Figure 5.5: *(a) P_d (b) Mean Absolute Error (c) Variance versus C/N0 for SinBOC(1,1) signal in single-path channel profile.*

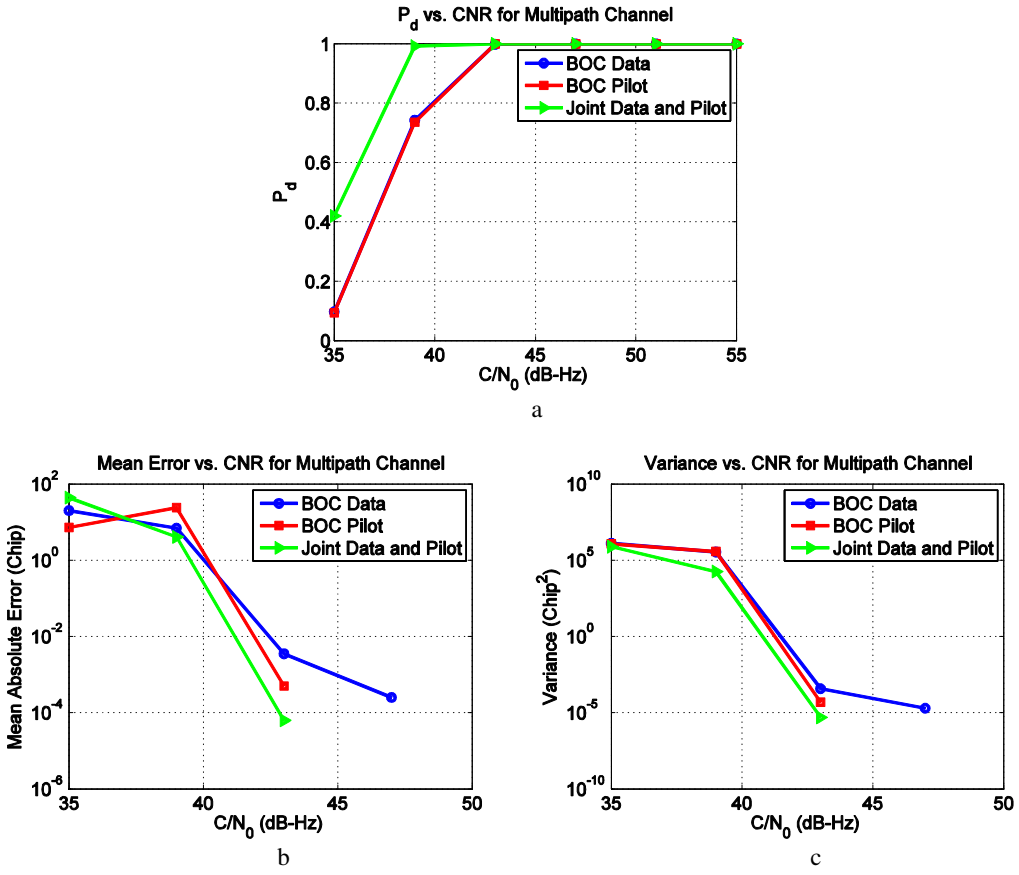

Figure 5.6: *(a) P_d (b) Mean Absolute Error (c) Variance versus C/N0 for BOC signal in multi-path channel profile.*

Figure 5.5 and 5.6 depict the plots for detection probability, mean error and variance of SinBOC(1,1) reference receiver for data-only, pilot-only and joint data and pilot channel for single and multi-path channel profiles, respectively. In multi-path channel, first path delay is 0 chips and second path delay is 0.35 chips.

In single-path scenario, joint data and pilot channel gives 3 dB better detection probability than data-only and pilot-only channel, respectively at P_d = 0.9, which is in accordance with the expected 3-dB losses in single-channel processing mode. It is worth noticing here that pilot-only channel is performing slightly better than the data-only channel. It has 0.04 dB better performance than data-only channel. Data channel contains navigation data and pilot channel has no data so that no bit transition occurs and this makes the reception of signal better than with data channel. Similarly, joint data and pilot channel gives 3dB better detection probability than data-only and 3.02 dB better detection probability than pilot-only channel in multi-path scenario. Pilot-only channel and data-only channel has similar performance in multi-path scenario at P_d = 0.90.

5.4.1. Data-Pilot Combinations for CBOC Reference Receiver

Same acquisition strategies were adopted for CBOC reference receiver in order to acquire the signal. Figures 5.7 and 5.8 show the plots of detection probability, mean error and variance for single-path and multi-path channel profiles, respectively. Here acquisition was performed using CBOC reference receiver.

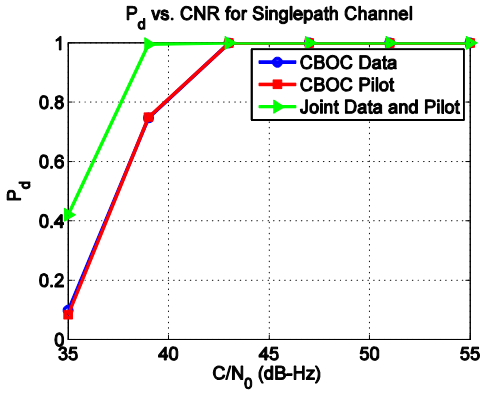

a

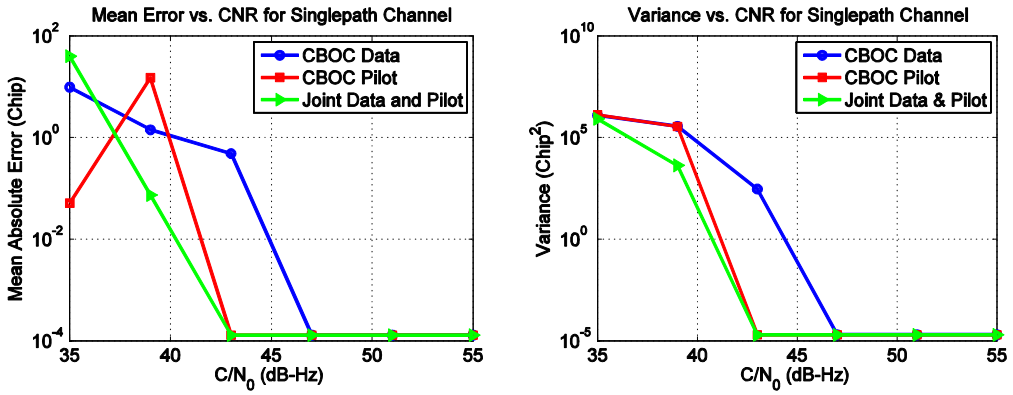

b c

Figure 5.7: *(a) P_d (b) Mean Absolute Error (c) Variance versus C/N0 for CBOC signal in single-path channel profile.*

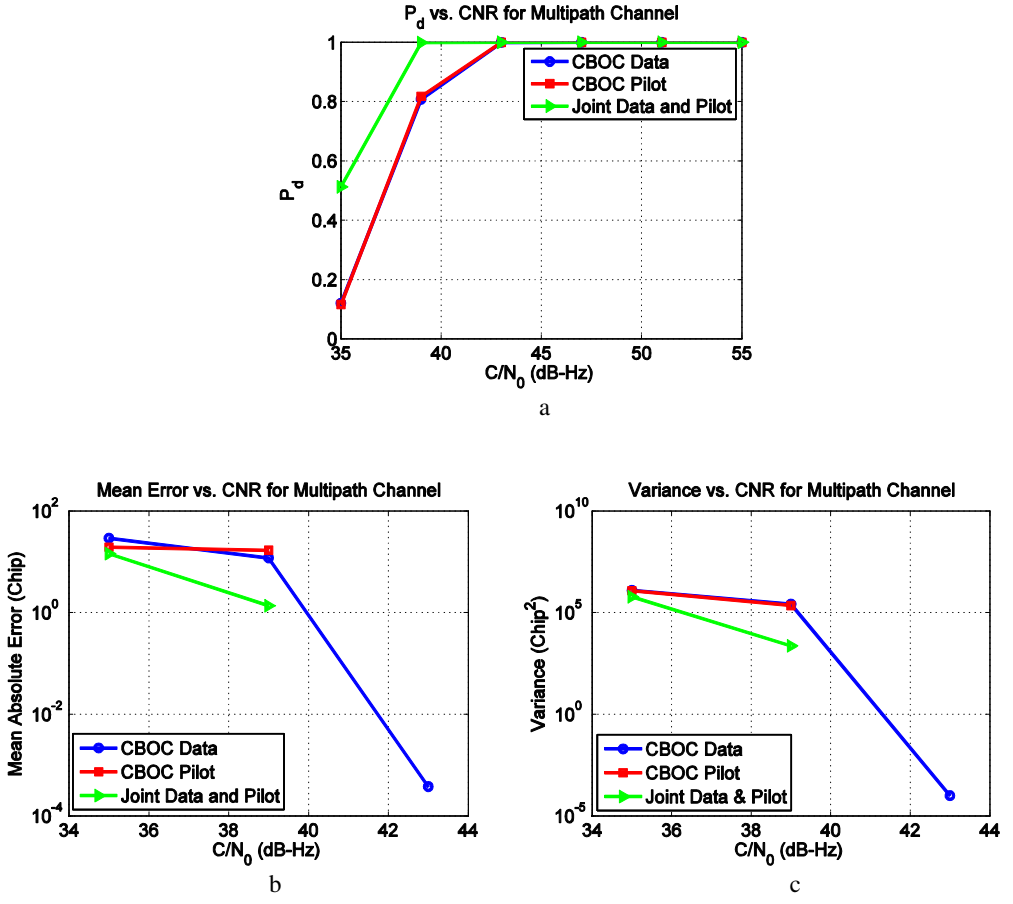

a

b c

Figure 5.8: *(a) P_d (b) Mean Absolute Error (c) Variance versus C/N0 for CBOC signal in multi-path channel profile.*

In single-path scenario, joint data and pilot channel gives 3.2 dB and 3.23 dB better detection probabilities than data-only and pilot-only channel, respectively, at $P_d = 0.9$. Pilot channel has better performance with CBOC reference receiver as well. Pilot channel has 0.03 dB better performance than data channel. The presence of the peak at the 39 dB is caused possibly due to the insufficient simulation time. Similarly, joint data and pilot channel gives 2.8 dB better detection probability than data-only and 2.9 dB better detection probability than pilot-only channel in multi-path scenario. Pilot channel has 0.1 dB better performance than data-only channel at $P_d = 0.9$ in multi-path scenario. It is worth noticing here that pilot-only channel is performing slightly better than the data-only channel. This is somehow counter-intuitive result, since the expectation would be that CBOC (-) signal has worse acquisition properties than CBOC(-) signal (to counter-balance the better tracking properties); however, the differences in detection probability are very small. Joint data and pilot channel combines all the significant power from data and pilot channel which ultimately improves the signal detection up to 3 dB extent and more in case of CBOC reference receiver.

5.4.2. Comparison between BOC and CBOC Reference Receiver

Figure 5.9 depicts combined graph of detection probability, mean absolute error and variance for data-only, pilot-only and joint data and pilot channel with SinBOC(1,1) and CBOC reference signal. The idea is to compare the performance of CBOC reference receiver in terms of detection performance of signal in multi-path scenario.

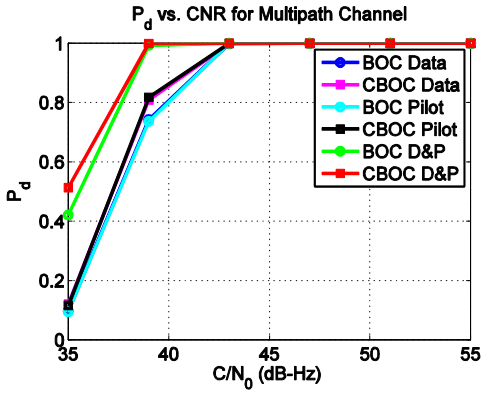

a

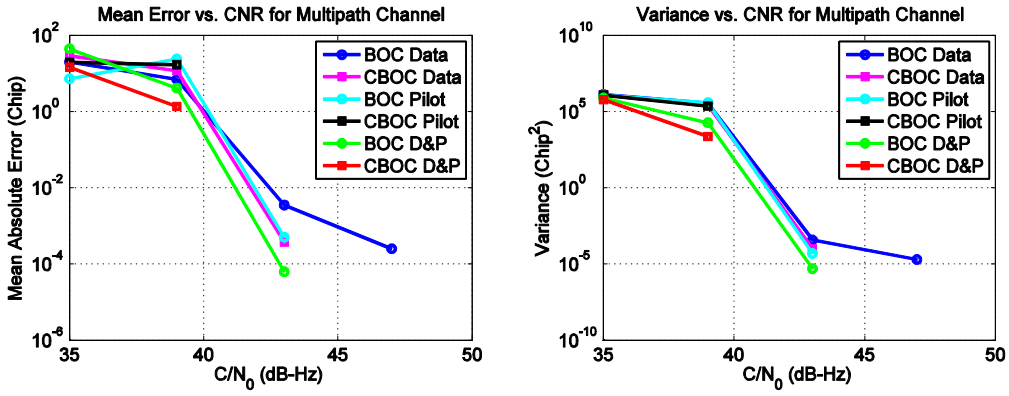

Figure 5.9: *(a) P_d (b) Mean Absolute Error (c) Variance versus C/N0 in multi-path channel profile.*

CBOC reference receiver has better performance than SinBOC(1,1) reference receiver. It is quite evident from the plots that CBOC joint data and pilot gives the best result among different acquisition strategies. CBOC joint data and pilot channel has 0.28 dB better detection probability than SinBOC(1,1) joint data and pilot channel at P_d = 0.8. Similarly, CBOC data-only has 1 dB better detection probability than SinBOC(1,1) data-only and CBOC pilot-only channel has 1.05 dB better detection probability than SinBOC(1,1) pilot-only channel. Mean absolute error and variance are also low for CBOC joint data and pilot.

Figure 5.10 shows the curve of joint data and pilot signals for single and multi-path channel profile for CBOC reference receiver. The idea is to see how much better is the result of detection probability in single-path compared to multi-path channel profile.

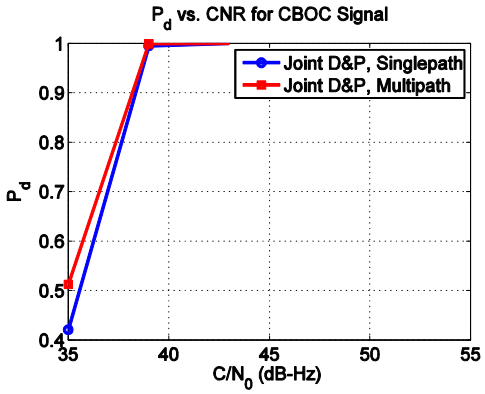

Figure 5.10: *P_d versus C/N0 for joint CBOC signal.*

In multi-path channel profile, first path delay is 0 chips and the second path delay is 0.35 chips. Joint CBOC data and pilot in single-path channel gives 0.05 dB better detection probability than in multi-path channel.

5.4.3. Choice of the Weighting Factor

In order to choose the best weighting factor for combining non-coherently the data and pilot channels, a study has been carried out and plots are available for detection probability and variance for different weighting factors.

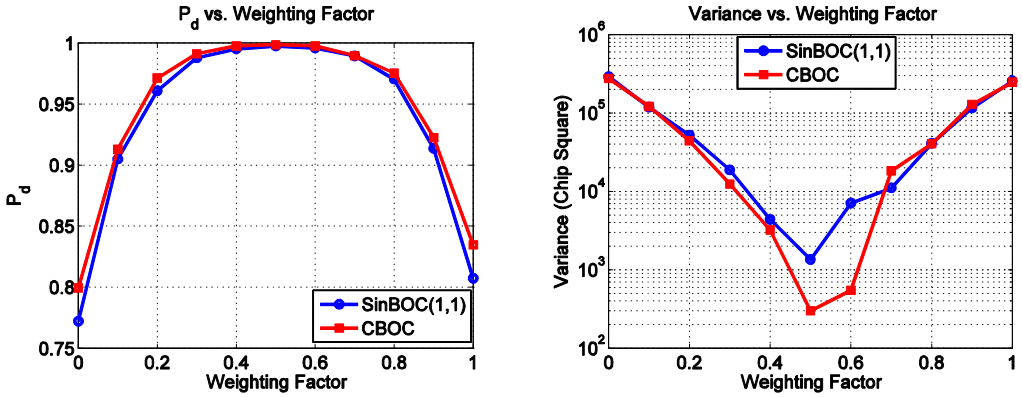

Figure 5.11: *(a) P_d (b) Variance versus Weighting Factor in multi-path channel.*

Figure 5.11 depicts the plots of detection probability and variance for both reference BOC and CBOC receiver, for various combinations of data and pilot. In this approach, non-coherent combining of data and pilot signals are used where received signal is correlated individually with the data and pilot local replicas. The correlation outputs are then multiplied with different weighting factors and finally summed to make the correlation output. It is evident from the graph that weighting factor = 0.5 gives the best detection probability among others. The same conclusion is reached by looking at the variance of the delay errors in the acquisition stage from Figure 5.11(b) (i.e., in terms of variance of the delay error, the optimum combining factor of 0.5 is clearly much better than the neighborhood values).

5.5 Detection Probability Versus time-bin Step

The effect of the time-bin step Δt_{bin} is depicted in Figure 5.12 for SinBOC(1,1) and CBOC signals. Here multi-path scenario was considered with first and second path

delay equal to 0.15 chip and 0.5 chip, respectively. C/N0 = 45 dB-Hz and the step for time-bin Δt_{bin} ranges from 1 sample to 1 chip. Figure 5.12 shows the plot of detection probability and variance against time-bin step.

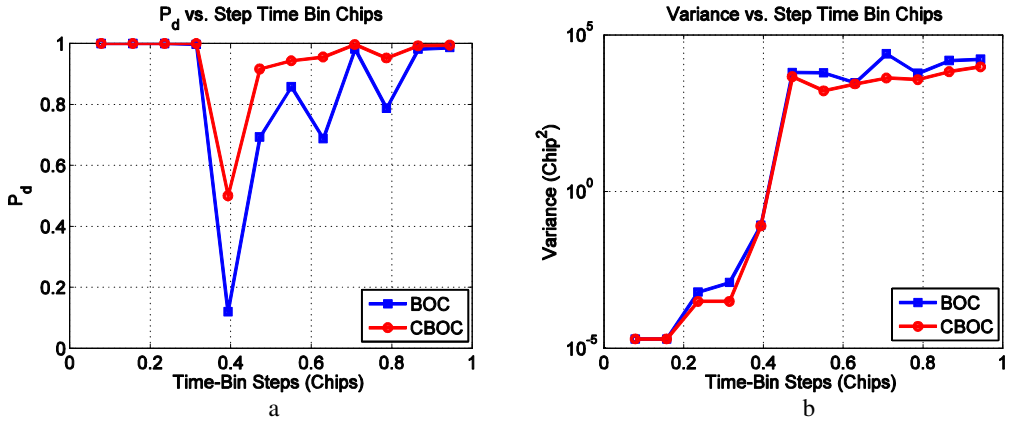

Figure 5.12: *(a) P_d (b) Variance versus time-bin steps for multi-path channel profile.*

The results reported so far in the acquisition stage were performed with a time-bin step of 1 sample, corresponding to 0.078 chips. However, the lower the time-bin step in the acquisition process is, the higher the mean acquisition time becomes, and therefore a higher time-bin step is usually preferable. As seen in Figure 5.12, the choice of the time-bin step has indeed a tremendous importance in the acquisition stage. It can be observed from the graph that steps higher than 4 samples are likely to give poor detection probability. At some higher steps, detection probability is still better especially for CBOC receiver but variance has higher values for such steps. As a rule of thumb, time-bin step for BOC modulated signal should be quarter of the width of the main lobe (i.e., 0.17 chips) to achieve better detection probability. This is matching also with GPS case, if we make the analogy that one quarter of the main correlation lobe in GPS C/A code is 0.5 chips, and this is the typical time-bin step used in the GPS acquisition [2].

5.6 Acquisition with Limited Bandwidth

This part describes the effect of front-end bandwidth on the signal acquisition of SinBOC(1,1) and CBOC reference receiver. For mass market receivers, limited front-end bandwidth design is the only possibility to reduce the manufacturing cost. In this approach, different front-end bandwidths are considered and plots of detection

probability across different ranges of C/N0 for BOC and CBOC receiver are depicted in Figure 5.13.

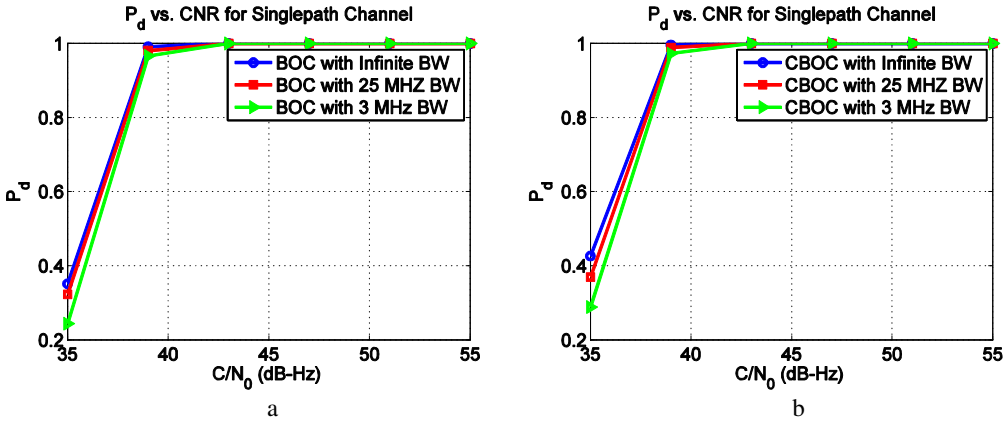

Figure 5.13: *P_d versus C/N0 (a) SinBOC(1,1) reference signal. (b) CBOC reference signal, double-sided bandwidth.*

It is obvious from the graph that the performance of BOC and CBOC receiver with infinite bandwidth is better in terms of detection probability. BOC receiver with infinite bandwidth has 0.04 dB better performance than receiver with 25 MHz front-end bandwidth and 0.2 dB better performance than receiver with 3 MHz front-end bandwidth. Similarly, CBOC receiver with infinite bandwidth has 0.1 dB better performance than receiver with 25 MHz front-end bandwidth and 0.2 dB better performance than receiver with 3 MHz front-end bandwidth. Both the receivers with 25 MHz front-end bandwidth have slightly better performance than receivers with 3 MHz front-end bandwidth. The choice of 25 MHz front-end bandwidth is an expensive choice for mass market receiver and receiver with 3 MHz front-end bandwidth has more or less the same performance in terms of detection probability. Thus, receiver with 3 MHz front-end bandwidth is a suitable choice for mass market receiver design.

5.7 Impact of the Threshold

The effects of choosing different acquisition threshold are discussed in this section. Figure 5.14 (a) depicts the plot of detection probability (i.e., P_d) with different acquisition threshold across different C/N0 values and impact of choosing different acquisition threshold are presented in Figure 5.14 (b) in terms of false alarm (i.e., P_{fa}). CBOC reference receiver was used here. Time-bin step Δt_{bin} = 1 in the acquisition unit.

Code delay error is computed within 0.175 chips. First path delay is 0 chips and the second path delay is 0.35 chips. Infinite front-end bandwidth was considered here.

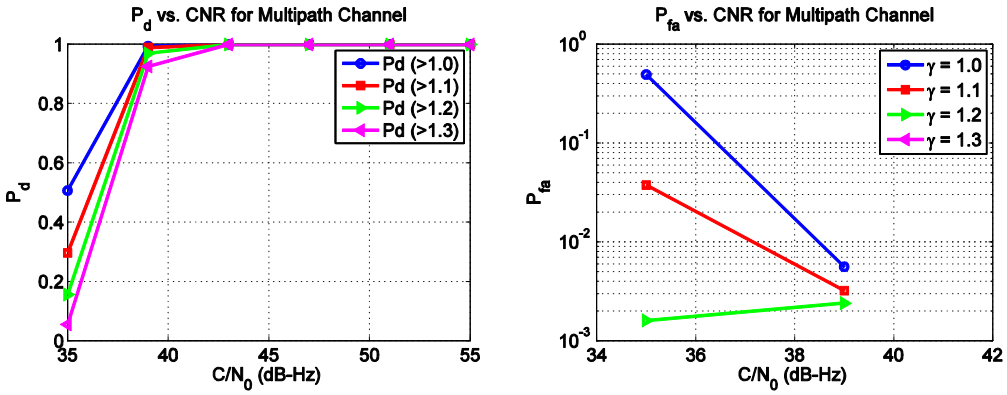

Figure 5.14: *(a) P_d versus C/N0 with CBOC reference signal. (b) P_{fa} versus C/N0 with CBOC reference signal.*

It is very important to choose suitable acquisition threshold in order to detect the signal properly. It can be observed from the graph that, if the detection probability is set too low, for example, when threshold, $\gamma = 1$, the probability of detection (i.e., P_d) increases (blue curve in Figure 5.10(a)) but on the other hand the probability of false alarm (i.e., P_{fa}) increases as well (blue curve in Figure 5.10(b)). In the same way, if detection threshold is set too high i.e., $\gamma = 1.3$, P_{fa} decreases (P_{fa} is zero in this case) but at the same time P_d decreases as well (pink curve in Figure 5.10(a)). The choice of a suitable detection threshold γ has great importance in the acquisition process. In our simulation model, acquisition threshold is set to 1.27.

5.8 Switching Architecture Simulation Results

Figure 5.15 depicts the plot of detection probability for switching architecture model in single-path channel profile. It is clearly evident from the graph that the performance of CBOC reference receiver with different switching time is significantly worse than the one without switching. The red curve which is the P_d without switching time is giving around 5 dB better performance than those with switching time. However, based on the simulation results, the best switching time is 2 ms.

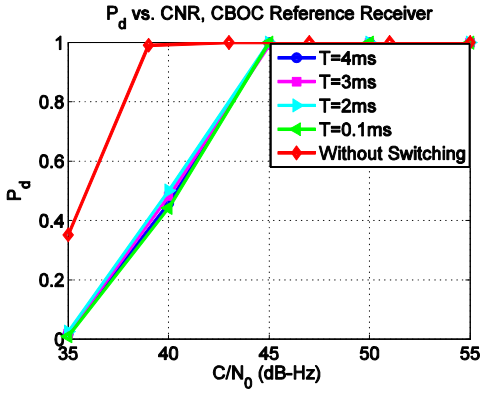

Figure 5.15: *P_d versus C/N0 with different switching time.*

Chapter 6

Matlab-Based Simulation Results

This chapter deals with the simulation results achieved from the Matlab model. The Matlab model consists of the transmitter part, the channel part and the receiver acquisition unit. This chapter starts by specifying the difference between Matlab and Simulink models then presenting the results for detection probability and root mean squared error of CBOC and BOC signals for single-path and then multi-path channel profiles. Further plots deal with the comparison of data, pilot and joint data-pilot channel in terms of detection probability and root mean squared error. Last section describes the impact of choosing different detection threshold and maximum delay error in terms of detection probability for CBOC reference receiver.

6.1 Difference between Matlab and Simulink Model

Figure 6.1 shows the simplified block diagram of Matlab model. The transmitter block is implemented based on CBOC modulation i.e. combination of CBOC('+') and CBOC('-') modulated signals. The E1-B signal is the CBOC('+') modulated signal with navigation data and E1-C is the CBOC('-') modulated signal without navigation data (pilot channel). Similarly, in the Simulink model, the E1 transmitter block is also implemented based on CBOC modulation. In the channel block of Matlab model, Nakagami-*m* fading channel is used, where multi-path fading channel environment affects the transmitted signal via specific fading coefficients, whereas in Simulink model, static channel with AWGN is used. The receiver block of Matlab model is based on two receiver options: one which uses a reference SinBOC(1,1)-modulated code for CBOC based transmitted signal, another one which uses a reference CBOC (combination of CBOC('+') and CBOC('-')) modulated code for the transmitted signal. The operation of Simulink based receiver is different with what we have in Matlab model i.e. SinBOC(1,1)-modulated code is correlated individually with E1-B and E1-C

channel for BOC reference receiver. A reference CBOC(+)-modulated code is correlated with E1-B and a reference CBOC(-)-modulated code is correlated with E1-C channel for CBOC reference receiver. In Matlab-based model, transmitted signal is correlated with SinBOC(1,1) reference code and CBOC reference code for SinBOC(1,1) and CBOC reference receiver, respectively.

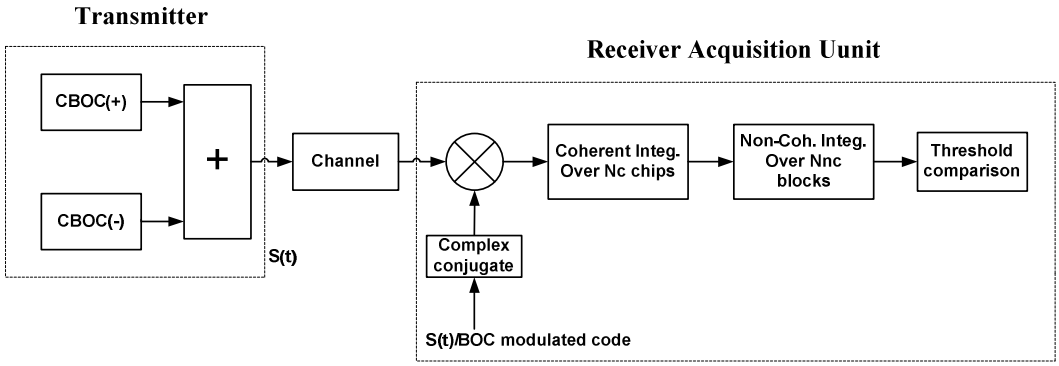

Figure 6.1: *Block diagram of Matlab model with BOC/CBOC reference receiver.*

Matlab model is a simplified version developed for the faster algorithmic development and analysis, whereas Simulink model is more realistic from implementation point of view. Other parameters which are different in both the model are reported in Table 6.1.

Table 6.1: *Comparison between Simulink and Matlab simulation parameters.*

Parameters	**Matlab Model**	**Simulink Model**
Spreading factor (S_F)	41 chips	1023 chips
No. of frequency bins	2	5
Search strategy	Serial search	Parallel search
Time-bin step	0.020 chip	0.078 chip
Sampling frequency	49.10 MHz	13 MHz
Correlation type	Time domain	Frequency domain
Coherent Integration time (N_c)	20 ms	4 ms

6.2 Simulation Parameters

In the simulations, the time-bin length 'Δt_{bin}' was 0.020 chips that comes in fact from 1/Ns/ N_{BOC}, N_{BOC} = 12 for CBOC and the oversampling factor N_s for the received signal was 4 samples per BOC/MBOC interval. A coherent integration time, Nc = 20 ms was used, followed by non-coherent integration on Nnc = 1 block. The multi-path delay spacing is 0.35 chips and the amplitude of the second path is 1 dB lower than the first one. The PRN codes length or spreading factor, S_F = 41 was considered, smaller spreading factor was used in order to speed up the simulation (however, since in GPS and Galileo, S_F =1023 chips, our Matlab model is only an approximation of the real system, and the purpose here was to study the impact of those simplifying approximations on the performance analysis). The statistics were computed for N_{rand} = 500 points for each Carrier to Noise Ratio (CNR or C/N0) value. The false alarm probability, $P_{fa} = 10^{-3}$ and acquisition threshold equal to 1.3 was used in the simulations. The code delay error is compared with the threshold equal to 0.175 chips which is one-fourth of the width of the main lobes of ACF envelope of CBOC (this is the same as in Simulink model). The root mean square error values used in the statistics are expressed in meters and they are computed as:

$$RMSE = \sqrt{\frac{\sum_{i=1}^{N_{obs}} \left(\hat{\tau}^{(i)}_{LOS} - \tau^{(i)}_{LOS}\right)^2}{N_{obs}}} cT_c \tag{5.4}$$

where c is speed of light and other parameters have the same meaning as in formula 5.1.

6.3 Comparison of SinBOC(1,1) and CBOC Reception

Figure 6.2 compares the performance of SinBOC(1,1) reference receiver with joint CBOC reference receiver in terms of detection probability in single-path channel profile, root mean squared error is also depicted in the figure. The SinBOC(1,1) reference receiver gives 0.4 dB better detection probability than CBOC reference receiver at P_d = 0.8. RMSE errors for SinBOC(1,1) reference code is also less than those of CBOC reference code.

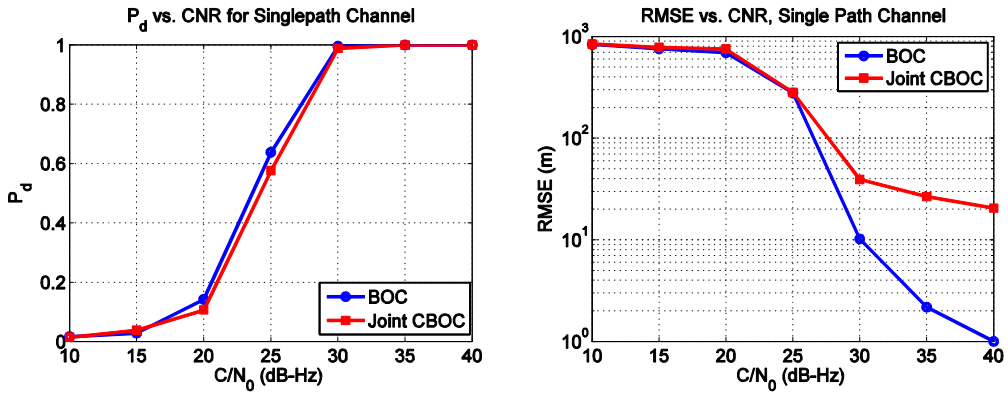

Figure 6.2: *(a) P_d (b) Root Mean Squared Error versus CNR for single-path channel.*

Figure 6.3 shows the plot of detection probability versus CNR of SinBOC(1,1) and CBOC reference receiver for single-path channel achieved from Simulink model. The performance deterioration of CBOC signal in the plot achieved by Matlab model is clearly visible. It is due to the different operation of Matlab based receiver as explained in Section 6.1. Another reason is the use of different codes for Matlab and Simulink model i.e. in Matlab model, simple pseudorandom codes have been used for CBOC modulation but in Simulink model primary and secondary codes for E1-B and E1-C signals have been used exactly according to SIS ICD documents [1].

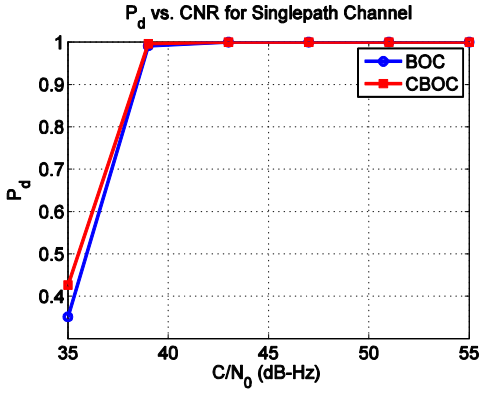

Figure 6.3: *P_d versus C/N0 for single-path channel.*

6.4 Comparison of Data-only, Pilot-only and Joint Data-pilot Processing with BOC Reference Receiver

Figure 6.4 depicts the plots of detection probability versus CNR for single-path and multi-path channel profiles for reference SinBOC(1,1) receiver achieved from Matlab model. The transmitted signal is based on joint CBOC modulation i.e., non-coherent

combining of CBOC('+') and CBOC('-'). It can be analyzed from the graph that, in single-path, data-only channel has 0.35 dB better performance than joint channel and 0.04 dB better performance than pilot-only channel. In multi-path channel, joint channel provides 0.6 dB better performance than pilot-only and 0.08 dB better performance than data-only channel.

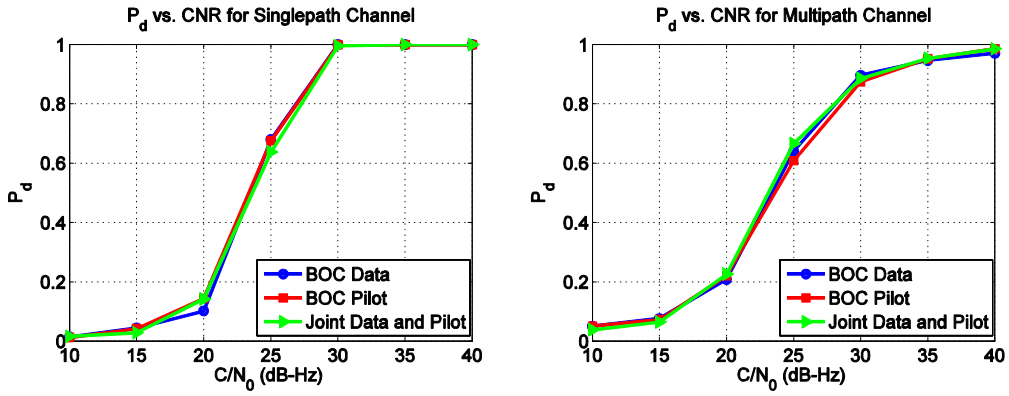

Figure 6.4: *P_d versus CNR with SinBOC(1,1) reference receiver (a) single-path channel (b) multi-path channel.*

Figure 6.5 depicts the plots of P_d versus CNR for SinBOC(1,1) reference receiver achieved from the Simulink model. It can be clearly observed that pilot-only channel is performing slightly better than data-only channel in single and multi-path channel profiles which is not the case in Matlab model.

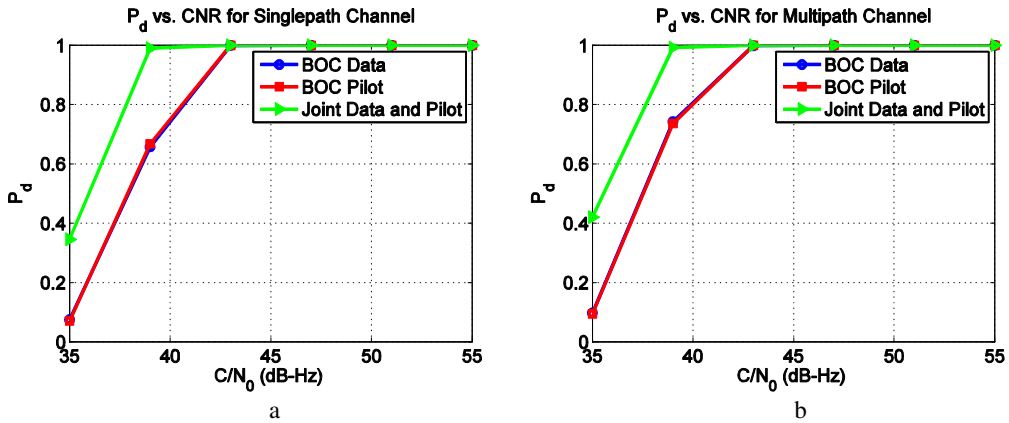

Figure 6.5: *P_d versus CNR with SinBOC(1,1) reference receiver (a) single-path channel (b) multi-path channel.*

6.5 Comparison of Data-only, Pilot-only and Joint Data-pilot Processing with CBOC Reference Receiver

Figure 6.6 depicts the plots of detection probability versus CNR for single-path and multi-path channel profiles for reference CBOC receiver obtained from Matlab model. The transmitted signal is based on joint CBOC modulation. It can be noticed from the graph that, data-only channel has 0.6 dB better detection performance than joint channel acquisition and 0.7 dB better performance than pilot-only channel at $P_d = 0.8$ in single-path scenario. In multi-path scenario, data-only channel has 0.3 dB better performance than joint channel and 1.1 dB better performance than pilot-only channel at $P_d = 0.8$.

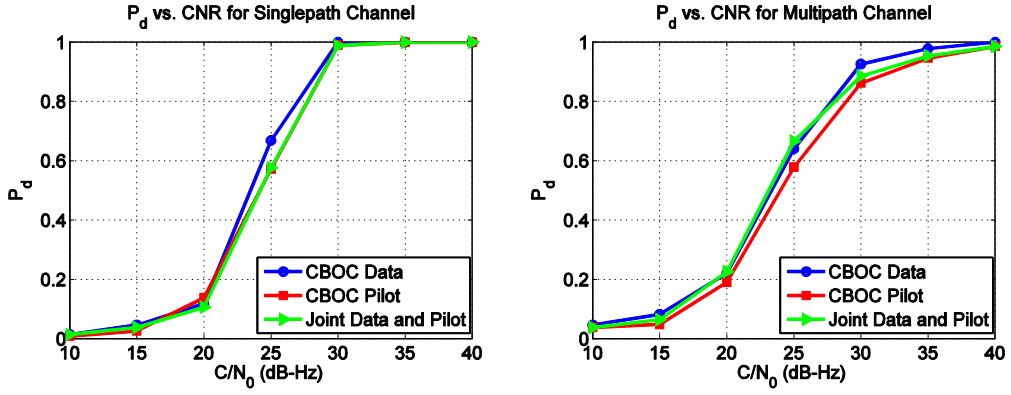

Figure 6.6: *P_d versus CNR with Matlab model (a) single-path channel (b) multi-path channel.*

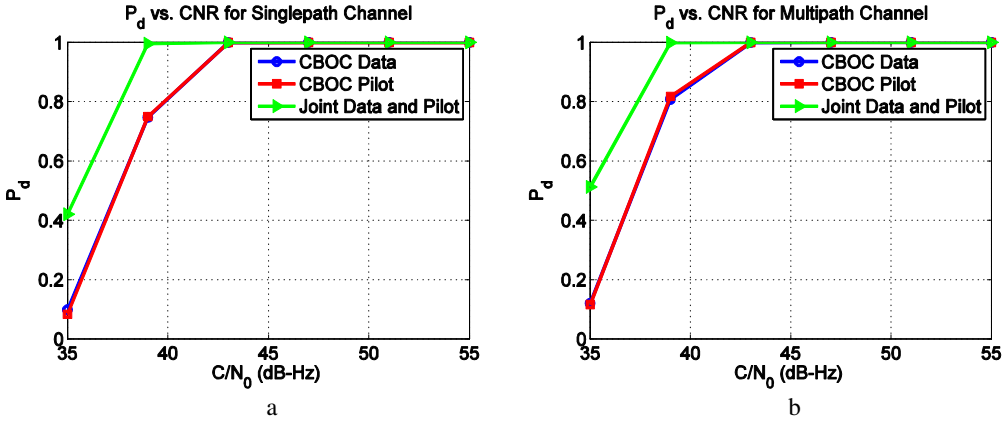

Figure 6.7: *P_d versus CNR with Simulink model (a) single-path channel (b) multi-path channel.*

Figure 6.7 shows the plots of P_d versus CNR for CBOC reference receiver achieved from the Simulink model. It can be clearly observed that pilot-only channel has slightly

better performance than those of data-only channel in single-path and multi-path channel profiles.

We remark that in the Simulink model, pilot-only channel was slightly better than data-only channel and joint channel was giving the best detection performance among different acquisition strategies. The reason for this contradictory result is due to the different simulation parameters as reported in Table 6.1 and different operations of Simulink and Matlab receiver.

6.6 Impact of Acquisition Threshold

The effect of choosing different acquisition thresholds on the detection performance of the CBOC receiver is discussed here. Figure 6.8 shows the plot of P_d versus CNR for different threshold. Multi-path channel scenario is considered here and the code delay error is fixed to 0.175 chips, joint CBOC reference receiver is used here. It can be easily observed from the plots that as the acquisition threshold is decreasing, P_d is decreasing as well. The choice of the acquisition threshold is indeed a non-trivial task, for example, if the acquisition threshold is set too low, the probability of detection (i.e., P_d) increases but at the same time the probability of false alarm (i.e., P_{fa}) increases as well. Similarly, if threshold is set too high, P_{fa} decreases, on the other hand P_d decreases as well which is quite obvious from the graph presented below.

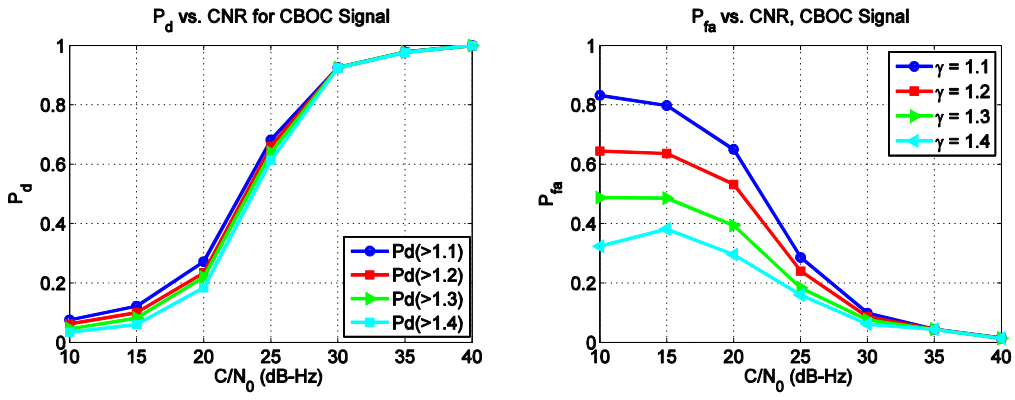

Figure 6.8: *(a) P_d (b) P_{fa} versus CNR with different acquisition thresholds.*

6.7 Impact of Maximum Delay Error

In Figure 6.9, a comparison among the P_d of joint CBOC reference receiver with different code delay error is depicted. P_{fa} is fixed to 10^{-3}. The detection probability is computed by the same formula as stated in Eq. 5.1.

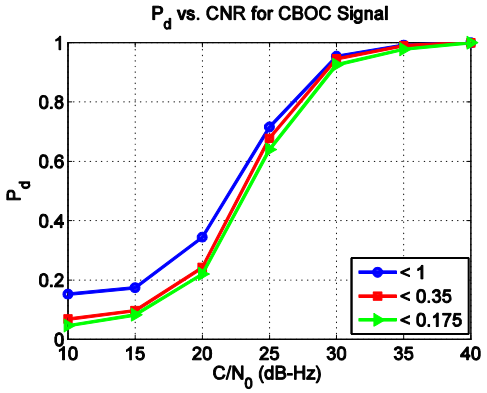

Figure 6.9: *P_d versus CNR with different delay error.*

It is evident from this comparison that when the delay error is higher, maximum detection rates can be achieved e.g., when delay error is 1 chip, higher detection probability is obtained. In order to detect the signal properly for the tracking stage, the maximum delay error must not be more than 0.35 chips in case of CBOC signal (this is equal to half of the main lobe correlation width and defines the linear region of most delay tracking structures). As explained in the previous chapter, most of the CBOC signals energy is found within half of the width of the main lobe of auto-correlation function which is 0.35 chips so even smaller delay error should be adopted in order to detect the signal significantly.

6.8 Normalized ACFs of Reference BOC and CBOC Receiver

Figure 6.10 depicts the ACF curves of CBOC('+'), CBOC('-') and SinBOC(1,1) signals obtained by Matlab and Simulink model. The transmitted signal is based on joint CBOC modulation for both the Simulink and Matlab model. At the receiver, the reference code is CBOC('+'), CBOC('-') and SinBOC(1,1) for Simulink and Matlab model, respectively in plots 6.5(a), 6.5(b) and 6.5(c). It is to be noticed the very good match between the ACFs of Matlab and Simulink model.

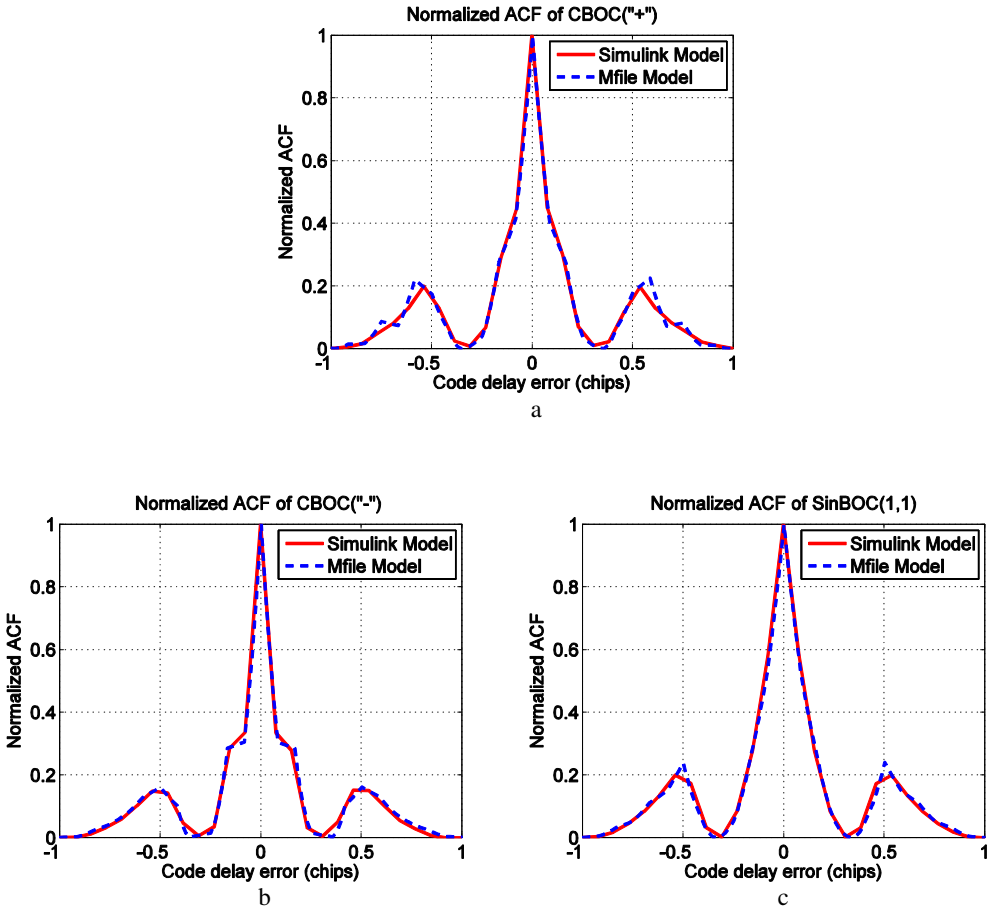

Figure 6.10: *Normalized ACF of (a) CBOC('+') (b) CBOC('-') and (c) SinBOC(1,1).*

Chapter 7

Conclusion and Further Research Issues

This chapter deals with the conclusions obtained from the simulation results and continuation of the research in the future.

7.1 Conclusions

The new Galileo OS signals introduce new challenges due to the longer spreading codes and require increased computational power as compared to GPS signals. However, the use of BOC modulated signals guarantees better performance against multi-path fading, and the presence of longer tired code helps the Galileo OS signals to have increased efficiency in indoor environment. In this thesis, a new acquisition unit based on CBOC reference code has been implemented in the basic Galileo Simulink model in order to investigate the performance of Galileo E1 OS signal with two receiver types: a reference CBOC receiver and a reference SinBOC(1,1) receiver. From the simulation results, it was shown that the CBOC reference receiver has slightly better performance than SinBOC(1,1) reference receiver mainly due to a higher transition rate brought by the BOC(6,1).

The E1 OS signal is composed of two channels: the data and the pilot channel. The former carries the navigation data whereas the latter is a data-free channel. This new composition of E1 signal allows one to choose different techniques in order to acquire the signal. Three different approaches were used for acquiring the received signal: data-only channel, pilot-only channel and joint data and pilot channel. A study was also carried out in order to find the best weighting factor for combining data and pilot channels. Based on the simulation results, it has been observed that acquisition with individual channel is not the best approach to acquire the signal. Joint data and pilot

channels combine all the significant power from data and pilot channel which ultimately improves the signal detection up to 3 dB in case of both the receivers. However, if only one channel has to be used, the acquisition with pilot-only channel has the best performance with both SinBOC(1,1) and CBOC reference receiver.

The acquisition with pilot-only channel leads towards new findings that acquisition based on CBOC(+) modulated signal is no better than the acquisition based on CBOC(-) signal. Moreover, such analysis has not been done before in the literature, to the best of the authors' knowledge. It was also shown that pilot-only channel gives better performance than data-only channel with both SinBOC(1,1) and CBOC reference receiver.

Another issue in the acquisition stage of Galileo OS signal is the presence of additional peaks within ± 1 chip interval around the main lobe. The steps should be chosen quite carefully in order to detect the signal properly. The impact of acquisition on time-bin steps was analyzed and it was shown that the time-bin step for SinBOC(1,1) modulated signal should be quarter of the width of the main lobe (i.e., 0.175 chips) to achieve better detection probability.

Under infinite bandwidth case, CBOC reference receiver has clearly better performance than SinBOC(1,1) reference receiver, however, the difference in performance is rather small (less than 0.5 dB) in the acquisition stage. This difference is no longer visible in the narrowband case, where a SinBOC(1,1) reference receiver is the best solution. From mass market receiver point of view, lower front-end bandwidth design is preferable due to low cost and based on the results, 3 MHz front-end bandwidth has proposed for mass market receiver design.

From the simulation based on acquisition threshold, it was observed that lower detection threshold increases the probability of detection but increases the probability of false alarm. Similarly, if detection threshold is chosen too high, probability of false alarm decreases but probability of detection decreases. Thus, $\gamma = 1.3$ is the best acquisition threshold among different values used during simulation.

The performance of switching architecture model has been reported and it was shown to perform worse in terms of detection probability compared to those without switching, but switching time, 2 ms gives the best result among different switching time.

7.2 Future Work

The acquisition methods proposed in this research were applied for Galileo OS signal which operates at E1 carrier frequency. However, there are other frequencies like E5a and E5b where Galileo OS signals are going to operate in future. They have different frequency bands, modulation schemes and shapes of the auto-correlation function. As such, the techniques proposed during this research would need to be adapted and investigated.

The Simulink based simulator can be further developed with respect to real Galileo receiver with the addition of some new blocks, such as Low Noise Amplifier (LNA), Analog to Digital Converter (ADC) and etc.

With the development and modernization of new GNSS signals, new horizons are opening in terms of signal combinations at the same frequency and at different frequencies. It is anticipated that once Galileo system will be fully operational, most of the receiver will be sold with both GPS and Galileo compatible. Thus, further efforts can be carried out to develop a dual band GNSS receiver.

References

[1] Galileo Open Service, Signal in Space Interface Control Document, OS SIS ICD (2008), Draft 1.

[2] E. D. Kaplan and C. J. Hegarty. Understanding GPS: Principles and Applications. Artech House, 2nd edition, 2006.

[3] F. Dovis, L. L. Presti, M. Fantino, P. Mulassano, and J. Godet. Comparison between Galileo CBOC Candidates and BOC(1,1) in Terms of Detection Performance. In International Journal of Navigation and Observation, 2008.

[4] Daniele Borio and Letizia Lo Presti. Data and Pilot Combining for Composite GNSS Signal Acquisition. Hindawi Publishing Corporation, International Journal of Navigation and Observation, Volume 2008, Article ID 738183, 12 pages.

[5] The European Space Agency (ESA official website). Available via <http://www.esa.int>, referred July 17, 2007.

[6] Official GNSS Magazine. Available via <http://www.insidegnss.com>.

[7] The Global Positioning System (GPS official website). Available via <www.gps.gov>.

[8] Global Navigation and Positioning (GPS world official website). Available via <http://www.gpsworld.com >, referred January 19, 2009.

[9] Satellite System GLONASS Status and Plans. Information Satellite System, available via < http://www.oosa.unvienna.org>.

[10] G. W. Hein, J. Godet, J. L. Issler, J. C. Martin, P. Erhard, R. L. Rodriguez, and T. Pratt. Status of Galileo Frequency and Signal Design. In CDROM Proceedings of ION GPS, September, 2002.

[11] G. W. Hein, M. Irsigler, J. A. A. Rodriguez, and T. Pany. Performance of Galileo L1 Signal Candidates. In Proceedings of The European Navigation Conference (ENC- GNSS), 2004.

[12] M. Z. H. Bhuiyan. Analyzing Code Tracking Algorithms for Galileo Open Service Signal. Master's Thesis, Department of Communications Engineering, Tampere University of Technology, Tampere, Finland, August, 2006.

[13] COSPAS-SARSAT web site. International Satellite System for Search and Rescue. Available via <http://www.cospas-sarsat.org>. Referred May 12, 2006.

[14] Galileo Joint Undertaking - The European Programme for Global Navigation Services. Available via <http://www.galileoju.com>.

[15] K. M. N. Islam. CNR Estimation and Indoor Channel Modeling of GPS Signals. Master's Thesis, Department of Communications Engineering, Tampere University of Technology, Tampere, Finland, March, 2008.

[16] G. W. Hein, J. A. Avila-Rodriguez, S. Wallner, A. R. Pratt, J. Owen, J. L. Issler, J. W. Betz, C. J. Hegarty, Lt S. Lenahan, J. J. Rushanan, A. L. Kraay, and T. A. Stansell. MBOC: The New Optimized Spreading Modulation Recommended for Galileo L1 OS and GPS L1C. In Position, Location, And Navigation Symposium, 2006 IEEE/ION, pages 883– 892, April, 2006.

[17] J. W. Betz. The Offset Carrier Modulation for GPS modernization. In Proceedings of ION National Technical Meeting (ION-NTM '99), pages 639–648, January, 1999.

[18] Capt. B. C. Barker, J. W. Betz, J. E. Clark, J. T. Correia, J. T. Gillis, S. Lazar, Lt. K. A. Rehborn, and J. R. Straton. Overview of the GPS M Code Signal. In Proc. of Institute of Navigation National Tech. Meeting: Navigating into the New Millennium, pages 542–549, January, 2000.

[19] Raghavan SH, Holmes JK. Modeling and Simulation of Mixed Modulation Formats for Improved CDMA Bandwidth Efficiency. In Proceedings of Vehicular Technology Conference 2004; 6: 4290–4295.

[20] E. S. Lohan, A. Lakhzouri, and M. Renfors. Binary-Offset-Carrier Modulation Techniques with Applications in Satellite Navigation Systems. Wireless Communications & Mobile Computing, 7(6):767–779, August, 2007.

[21] G. W. Hein, J. A. Avila-Rodriguez, L. Ries, L. Lestarquit, J. L. Issler, J. Godet, and A. R. Pratt. A Candidate for the Galileo L1OS Optimized Signal. In Proceedings of ION2005, Long Beach, California, September, 2005.

[22] J. A. Avila-Rodriguez, S. Wallner, G. Hein, E. Rebeyrol, O. Julien, C. Macabiau, L. Ries, A. DeLatour, L. Lestarquit, and J. Issler. CBOC -An Implementation of MBOC. In First CNES Workshop on Galileo Signals and Signal Processing, Toulouse, France, October, 2006.

[23] E. Pajala. Code-Frequency Acquisition Algorithms for BOC Modulated CDMA Signals with Applications in Galileo and GPS Systems. Master's Thesis, Department of Communications Engineering, Tampere University of Technology, Tampere, Finland, August, 2005.

[24] M. Katz. Code Acquisition in Advanced CDMA Network. PhD Thesis, University of Oulu, Oulu, Finland, 2002.

[25] Vasu Chakvarthy, James Tusi and David Lin. Software GPS Receiver. Air force Research Laboratory, Wright Patterson Air Force Base, VeriHIan, Dayton, Ohio, 2001.

[26] F. V. Diggelen and C. Abraham. Indoor GPS Technology. Presented at CTIA Wireless agenda, Dallas, Texas, May 2001.

[27] T. S. Rappaport. Wireless Communications: Principles and Practice. Prentice Hall, 1996.

[28] Kai Borre- A Software-Defined GPS and Galileo Receiver.

[29] Carl Baum and Venugopal Veeravalli. Hybrid Acquisition Schemes for Direct Sequence CDMA Systems. In Proc. of ICC 94, SUPERCOMM/ICC '94, Conference Record, Serving Humanity Through Communications. IEEE International Conference, volume 3, pages 1433–1437, May, 1994.

[30] E. S. Lohan, A. Lakhzouri, and M. Renfors. Selection of the Multiple-Dwell Hybrid Search Strategy for the Acquisition of Galileo Signals in Fading Channels. In Personal and Indoor Mobile Radio Communications (PIMRC), volume 4, pages 2352–2356, Barcelona, Spain, September, 2004.

[31] Bub- Joo Kang, Hyung-Rae Park and Youngnam Han. Hybrid Acquisition in DS/CDMA Forward Link. In Proc. Of Vehicular Technology Conference 1977 IEEE 47th, Volume 3, pages 2123-2127, May, 1997.

[32] J. Betz and P. Capozza. System for Direct Acquisition of Received Signals. In US Patent Application Publication, US, April, 2004.

[33] N. Martin, V. Leblond, G. Guillotel, and V. Heiries. BOC (x,y) Signal Acquisition Techniques and Performances. In ION-GPS2003, Portland, OR, US, September, 2003.

[34] V. Heiries, D. Oviras, L. Ries, and V. Calmettes. Analysis of Non ambiguous BOC Signal Acquisition Performances. In ION-GNSS, Long Beach, CA, US, September, 2004.

[35] E. S. Lohan, A. Burian, and M. Renfors. Low-Complexity Acquisition Methods for Split-Spectrum CDMA Signals. Wiley International Journal of Satellite Communications, 2008.

[36] Md. Farzan Samad. Effect of MBOC Modulation on GNSS Acquisition Stage. Master's Thesis, Department of Communication Engineering, Tampere University of Technology, Tampere, Finland, March, 2009.

[37] M. K. Simon and M. S. Alouini. Digital Communication over Fading Channels. John Wiley & Sons, 2000.

[38] J. Jung. Implementation of Correlation Power Peak Ratio Based Signal Detection Method. In Proc. of ION GNSS 17th International Technical Meeting of the Satellite Division, Long Beach, CA, September, 2004.

[39] J. Pang, F. V. Graas, J. Starzyk, and Z. Zhu. Fast Direct GPS P-code Acquisition. GPS Solutions, 7(3):168–175, 2003.

[40] S. M. Kay. Fundamentals of Statistical Signal Processing, Vol 2: Detection Theory. Prentice Hall, 2000.

[41] W. D. Wilde, J. M. Sleewaegen, Andrew Simsky. New Fast Signal Acquisition Unit for GPS/Galileo Receiver. ENC GNSS 2006.

[42] E. S. Lohan, "Statistical Analysis of BPSK-like Techniques for the Acquisition of Galileo signals," in Proceedings of the 23rd AIAA International

Communication Systems Conference (IC-SSC ’05), Rome, Italy, September, 2005, CDROM.

[43] E. Pajala, E. S. Lohan, and M. Renfors. CFAR Detectors for Hybrid-Search Acquisition of Galileo Signals. In Proc. of the European Navigation Conference (ENC-GNSS ’05), Munich, Germany, July, 2005.

[44] Zhang Jie. Delay Trackers for Galileo CBOC Modulated Signals and Their Simulink-based Implementation. Master’s Thesis, Department of Communication Engineering, Tampere University of Technology, Tampere, Finland, February, 2010.